Date: May 3, 1999

DRAFT

From: Omar Moghaddam

To: Distribution

SUBJECT: Recent Particle and Turbidity Results at Hyperion

The enclosed report on particle counter measurements on the effluent supplied by Hyperion to the West Basin Water Recycling Plant clearly identifies the turbidity in this effluent as resulting from particles of greater than 7 μm in size. The correlation's between the densities of these particles and the turbidimeter readings are so consistently high as to leave no doubt of the identification, particularly since the particle counter also observed another population of smaller particles that is equally clearly seen not to be responsible for the observed turbidities.

This study is part of a larger effort by the Research Group to support the plant operators in the startup and optimization of the Hyperion Full Secondary. Other studies included a comparison of the turbidity to the conductivity of the effluent, a treatability study in which HTP secondary effluents and mixed liquor were tested with filters of differing pore sizes, and a hydraulic study that discovered a reverse hydraulic gradient between splitter boxes 3 and 4 in the water distribution system. However, the particle counter study has been more informative than any of these previous approaches.

If you have any questions call Rick Mayer or Reza Iranpour at 648-5066.

Cc: J. Mundine
S. Fan
H. Netto
D. Gumaer
Y.J. Shao
C. Turhollow
H. Rad
S. Oh
J. Winn
P. Cheng

Information: J. Wilson
J. Crosse
J. Langley
G. Garnas
T. Haug

RECENT PARTICLE AND TURBIDITY RESULTS AT HYPERION

EXECUTIVE SUMMARY

Measurements were made at the Hyperion pumping station with a particle counter from March 11 to March 23, 1999, to determine which particles cause the observed turbidities. The data were analyzed using time series plots, scatter plots, and correlation coefficients.

These show clearly that the observed turbidities are caused by a particle population covering the size range from about 7 μm to more than 15 μm. Hence, one would expect them to be removed by the filter systems that are specified to remove particles that are 5 μm or larger. However, turbidity peaks in the Title 22 effluent from West Basin imply that the incoming relatively large particles are in fact causing the observed turbidities in the Title 22 effluent.

There may be two possible explanations for this result: (a) that many of the relatively large particles are passing through the filters, contrary to the specification; (b) that after they leave the Hyperion pumping station the relatively large particles interact in some way with the subsequent pipes, pumps, and filters to produce particles that are less than 5 μm in size. Presently no information is available to determine which of these explanations is correct, and in fact they are not mutually exclusive.

Accordingly, we would recommend that particle counter observations be made at the West Basin plant, both before and after the filters, to determine the particle distributions at these points, and thereby to gain insight into the phenomena downstream from the location of the present set of measurements.

Introduction

These are the latest results of a study to understand the turbidities observed in the water supplied by Hyperion to the West Basin Water Reclamation Plant. These turbidities are higher than desired, and appear to be contributing to the frequent occasions when water from the West Basin plant exceeds the 2 NTU limit specified by Title 22. Simultaneous data from the particle counter and the turbidimeter at the Hyperion pumping station have been tabulated from March 11 to March 23, 1999, and subjected to several forms of analysis that show clearly that the observed turbidities are caused by a particle population covering the size range from about 7 μm to more than 15 μm.

Turbidimeters have been used for many years, they operate reliably, and their simplicity makes them inexpensive compared to particle counters, so they can be expected to remain the primary instruments for monitoring the particle content of water. However, understanding their limitations shows the benefit of using particle counters when more detailed information is needed.

These measurements have been made as part of a larger effort by the Research Group to support the plant in its effort to understand the turbidity problem in sufficient detail to make recommendations for overcoming it. For example, another study compared the turbidity to the conductivity of the effluent, in case a correlation between the two would allow a conductivity meter to provide easy and inexpensive estimates of turbidity variations. Simultaneous turbidity and conductivity data were recorded several times a day from several clarifiers for two weeks during the last half of January, 1999, but no usable relationship was found.

There was also a treatability study in which the HTP secondary effluents from clarifiers 1A and 2A, and the mixed liquor flowing to the clarifiers at IPS-6 were sampled at 1:00 PM on each of ten days in late January and early February. A filter with 8 μm pores usually reduced the turbidity to about half of its value in the unfiltered water, and a filter with 0.45 μm pores reduced the turbidity much more, but it was still almost always near or above 1 NTU.

Still another study showed a reverse hydraulic gradient between splitter boxes 3 and 4 in the water distribution system. Box 3 is downstream of box 4, so the head in box 3 would be expected to be lower, but on February 22, for example, it was several inches higher for several hours. This implies that some backflow is occurring in the distribution channel system, contrary to the intent of its design, and measures to stop the backflow appear desirable. However, the turbidity problem does not appear to be solely attributable to the backflow. The particle counter study has been more informative than any of these previous approaches.

Experimental Setup

The on-line laser particle counter (LPC) system was installed at the Hyperion Treatment Plant (HTP) next to the West Basin effluent pump building located on the southwest corner of the plant. A sample waste stream for the LPC was diverted from the inlet of an

existing Hach turbidimeter that monitors effluent from clarifier trains 1 and 2. ¼" O.D. tubing was used to connect the LPC inlet to this sample source and the LPC outlet to a drain. In the LPC the sample flows through a 750 μm by 750 μm optical flow cell. Each particle passing through the sensor generates a signal corresponding to its size.

In the MetOne™ Model PCX LPC system the laser measurement cell is interfaced through an RS-232 to RS-485 converter to a controlling computer running Vista Version 1.1. Vista is a proprietary Windows-based water quality software package that runs the complex functions of the LPC and stores the vast amounts of data collected. The system is in a NEMA 4x-rated enclosure, with a power supply and various cables and tubing needed for the cell and the electronic components. The entire system occupied only about three square feet of floor space.

For the present measurements the Vista program was commanded to assume a flow rate of 100ml/min through the cell, to take a reading every 10 minutes, and to classify the particles into six size ranges. The six ranges were 2-3 μm, 3-5 μm, 5-7 μm, 7-10 μm, 10-15 μm and 15-750 μm. These size ranges are set up based on state or federal regulations or the sizes corresponding to *Giardia* or *Cryptosporidium*..

Experimental Procedure

After a shakedown period and a one-week trial run the apparatus took samples for two weeks, from March 11 to March 23, 1999. Data were recorded every 10 minutes, 24 hours a day, in six separate size ranges totaling over 12,000 data points. The data were then transferred to a Microsoft Excel format and downloaded to a desktop PC for analysis.

Plant turbidity data from the same location were obtained for comparison with the particle counts. HTP uses a Bailey DCS for data gathering and storage. The PI-ProcessBook for Windows 95™ (Ver 1.30) was used as an interface to download data from Bailey to a desktop PC. These data were also stored in Excel format and analyzed as follows.

Time Series Plots

Time series plots have been prepared with the particle counter and turbidity results displayed on both linear and logarithmic vertical scales. These are attached respectively as parts (a) and (b) of each daily figure. Thus, Figure 1(a) is the linear plot of the data for

March 11 and Figure 1(b) is the logarithmic plot for the same day, and so on to Figures 13(a) and 13(b) for March 23.

As the larger particles are present in the smallest densities, the logarithmic scale emphasizes the variations in the densities of the larger particles more than the linear scale does, and provides the most emphatic visual demonstration of the extremely close correspondence between the turbidity readings and the densities of the larger particles.

Many other phenomena are evident in these plots. For example, there are prolonged periods during which the density in the 5-7 μm size channel is lower than the density in either the 3-5 μm channel or the 7-10 μm channel, implying that the density distribution as a function of particle size during these times was clearly bimodal. During the times that the 5-7 μm channel had higher readings, the differences from the densities in the 7-10 μm channel were usually small, indicating that the particles at least 7 μm in size formed a prominent shoulder on the side of the peak formed by the densities in the three channels in the interval from 2 μm to 7 μm. All of this is strong evidence that two particle populations are present.

Another form of evidence is the great difference between the behaviors shown in the different size channels. The 7-10 μm, 10-15 μm, and 15-750 μm size channels showed nearly perfect agreement in their fluctuations on both small and large time scales, so that these channels clearly were observing different portions of the same population of relatively large particles. Likewise, there were such strong correspondences between the 2-3 μm and 3-5 μm densities that these channels also were easily recognized as containing different portions of a population of small particles. However, the variations of the particle densities in the 2-5 μm interval did not agree with the density variations in the three largest size channels, but tended to vary oppositely with them, particularly in the period between 5:00 PM and 10:00 PM each day. The 5-7 μm size channel displayed an intermediate character, in the sense that earlier in the day it tended to fluctuate in step with the channels for the larger particles, but when the 2-3 μm and 3-5 μm count rates decreased around 6:00 PM, the 5-7 μm size channel did, too.

As the densities of the small particles varied more or less oppositely not only to the densities of the large particles but to the turbidity readings, it is clear that the response of the turbidimeter to the small particles was small or absent. Indeed, Figure 3 shows that notably low turbidities, approximately 3.3 NTU, were observed around noon of March

13, a day when the 3-5 μm density was in the range 6500-7000 particles/mL, but Figure 1 shows that the turbidity never dropped below 4.0 NTU on March 11, when the 3-5 μm density was 2000-3000 partcles/mL.

Although it is clear that two populations of particles are present, distributed around two differing mean sizes, the plots also show that the shapes of these distributions were subject to substantial changes, sometime lasting hours to days. As a particularly emphatic example, Figures 3(b) and 7(b) show that the ratio of the 3-5 μm density to the 2-3 μm density was much larger on March 13 than on March 17. Likewise, on most days rises in the total densities of the larger particles between 5:00 PM and 10:00 PM coincide with reductions of the ratio between the 7-10 μm density and the 10-15 μm density, and the 7-10 μm/15-750 μm density ratio.

Scatter Plots

To gain a more comprehensive view of the relationships between the turbidity readings and the densities in the size channels, scatter plots were prepared in which the turbidities were the vertical coordinates in each plot, but the densities for the respective size channels were the horizontal coordinates. The plots were arranged in two columns, so that reading down the columns gives the size channels in increasing order. These groups of plots are designated as part (c) of each daily figure, so that Figure 1(c) is the scatter plot for March 11, and the sequence continues to Figure 13(c) for March 23.

As expected from the nearly perfect correspondence, in the time series plots, between the variations of the turbidities and those of the densities in the 10-15 μm and 15-750 μm size channels for many days, the scatter plots for those densities versus the turbidities show very little departure from a single diagonal line that slopes up from left to right. Some of the plots of the densities in the 2-3 μm and 3-5 μm size channels versus the turbidities show a fairly clear diagonal line shape sloping down from left to right, and this also is as expected from the apparently opposite variation in some time series plots.

However, many of the scatter plots showed more complex behavior, some of which was not expected from the time series plots. For example, on March 13, the 7-10 μm density vs. turbidity plot in Figure 3(c) shows two upsloping straight lines diverging from each other to form a sideways V shape, and the 10-15 μm and 15-750 μm densities vs. turbidity show configurations that include nearly parallel diagonal lines. A hint of

parallel lines is also present in the corresponding scatter plots in Figure 11(c), for March 21.

More complex shapes are present in many of the scatter plots. The shift in the behavior of the 5-7 μm channel observed in the time series plots is reflected in the scatter plots by the presence of points arranged in two intersecting lines, one sloping down and one sloping up. This plot in Figure 3(c), for March 13, resembles an upside-down T, and the one in Figure 4(c), for March 14, resembles an L rotated around 100 degrees counterclockwise. The 3-5 μm plot for March 14 and both the 2-3 μm and the 3-5 μm plots in Figure 6(c), for March 16, show lines of positive and negative slopes, resembling distorted Vs that open to the left. The 3-5 μm plot in Figure 3(c) slightly resembles a fork with three unequal tines. The 2-3 μm and the 3-5 μm plots in Figure 1(c) for March 11 show two distinct groups of points and the corresponding plots in Figure 7(c) for March 17 show points arranged in a meandering line.

It is reasonable to interpret these groupings as reflecting changes in operating conditions during the day, and probably the changes in the particle distributions deduced from the time series plots. The BOD load on the plant changes inevitably, and operators or the control system may change the flows to the clarifiers according to changing influent flows. Identifying the times and operational parameters corresponding to these groupings might provide insight into physical, chemical or biological reasons for the behavior displayed in the plots.

Correlations

Correlation coefficients between turbidity and particle density were computed for each size channel for all the days, and the results are tabulated in Table 1. The high correlations for the 7-10 μm, 10-15 μm, and 15-750 μm size channels for most of the days are as would be expected from the nearly linear arrangements of points on the corresponding scatter plots. The few that are lower, such as for 7-10 μm on March 13, correspond to plots that depart from a linear configuration, but they all are consistent in showing positive correlations that are statistically significant at extremely high confidence levels, given the approximately 140 data points for each day used in the correlation calculation.

The smaller three size ranges display much more variable results. The 2-3 μm plots show the most frequent strong negative correlations, but these are still only five of the fourteen

days. It is clear from the scatter plots that the behavior in these size ranges often looks highly deterministic, but it is both much more variable from day to day than in the large size ranges, and usually not describable by a straight line. Hence, the great variation in the linear correlation coefficients and the frequent low correlations for these size ranges are also understood easily from the scatter plots.

Evidently, although there are individual days for which the correlations in the small size ranges have extremely high significance according to the conventional evaluation of confidence limits, these correspondences are only temporary. The most extreme case of unstable correlations occurs for the first two days of the data set, March 11 and 12. The correlations for the 2-3 μm, 3-5 μm, and 5-7 μm size channels are all greater than 0.7 on March 11 and less than -0.7 on March 12. In short, there is no significant long-term correlation between turbidity and the densities in these ranges, as shown by the averages of the correlations at the bottom of the table.

Conclusions and Recommendations

The turbidity readings at Hyperion have been shown to result from particles that are more than 5 μm in size. Hence, one would expect them to be removed by the filter system at the West Basin plant, which is specified to remove particles that are 5 μm or larger. However, the observed turbidity peaks in the Title 22 effluent occur after the arrival of turbidity peaks from Hyperion, with a lag matching the detention time in the West Basin filters, implying that the incoming relatively large particles are in fact causing the observed turbidities in the Title 22 effluent.

There are two obvious possible explanations for this result: (a) that many of the relatively large particles are passing through the filters, contrary to the specification; (b) that after they leave the Hyperion pumping station the relatively large particles interact in some way with the subsequent pipes, pumps, and filters to produce particles that are less than 5 μm in size. Presently no information is available to determine which of these explanations is correct, and in fact they are not mutually exclusive.

Accordingly, we recommend that particle counter observations be made at the West Basin plant, both before and after the filters, to determine the particle distributions at these points, and thereby to gain insight into the phenomena downstream from the location of the present set of measurements.

Fig. 1. Particle counts and turbidities of the influent to West Basin pumping station at HTP, 3/11/99.

(a) time series - linear scale

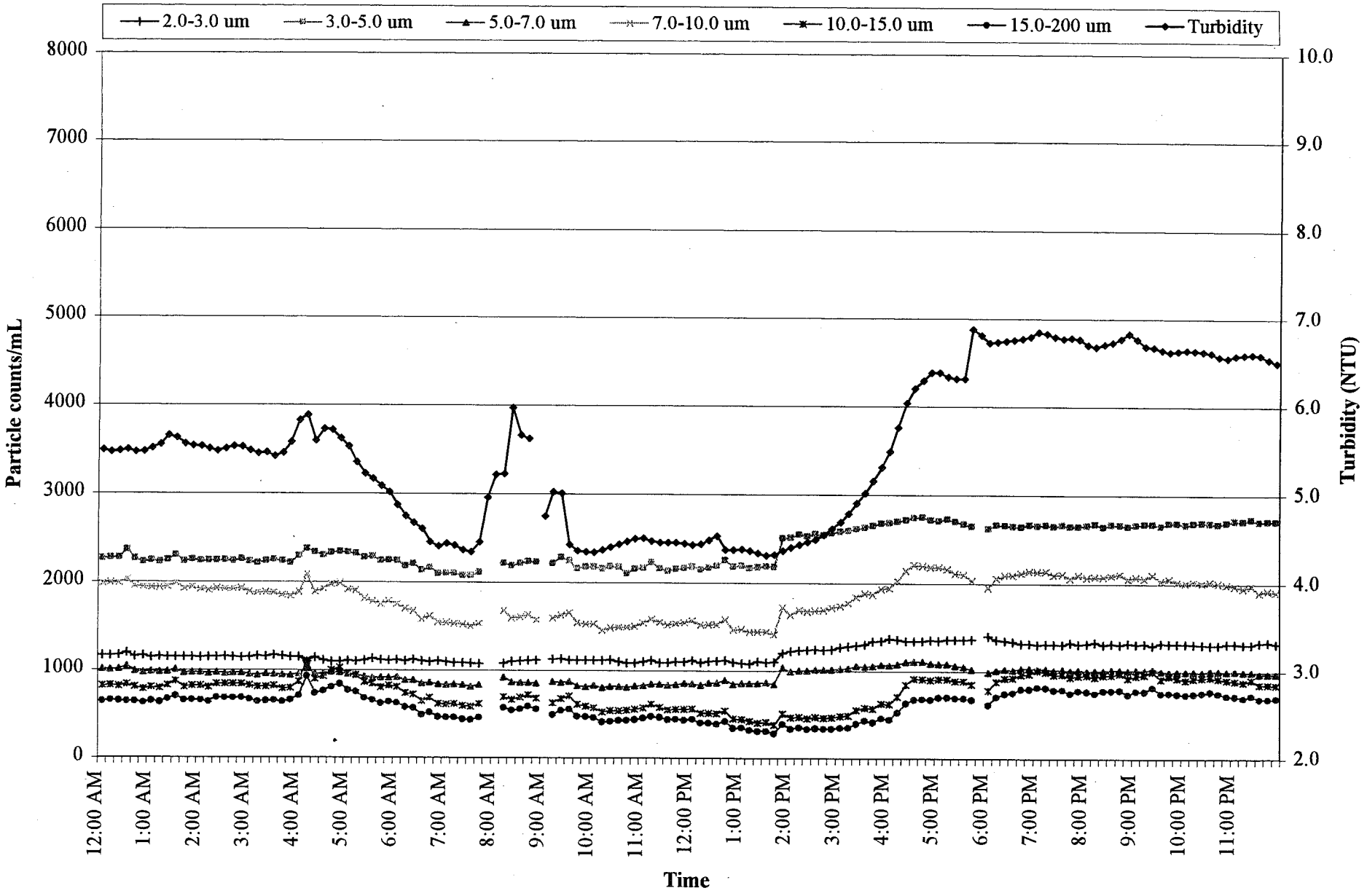

Fig. 2. Particle counts and turbidities of the influent to West Basin pumping station at HTP, 3/12/99.
(a) time series - linear scale

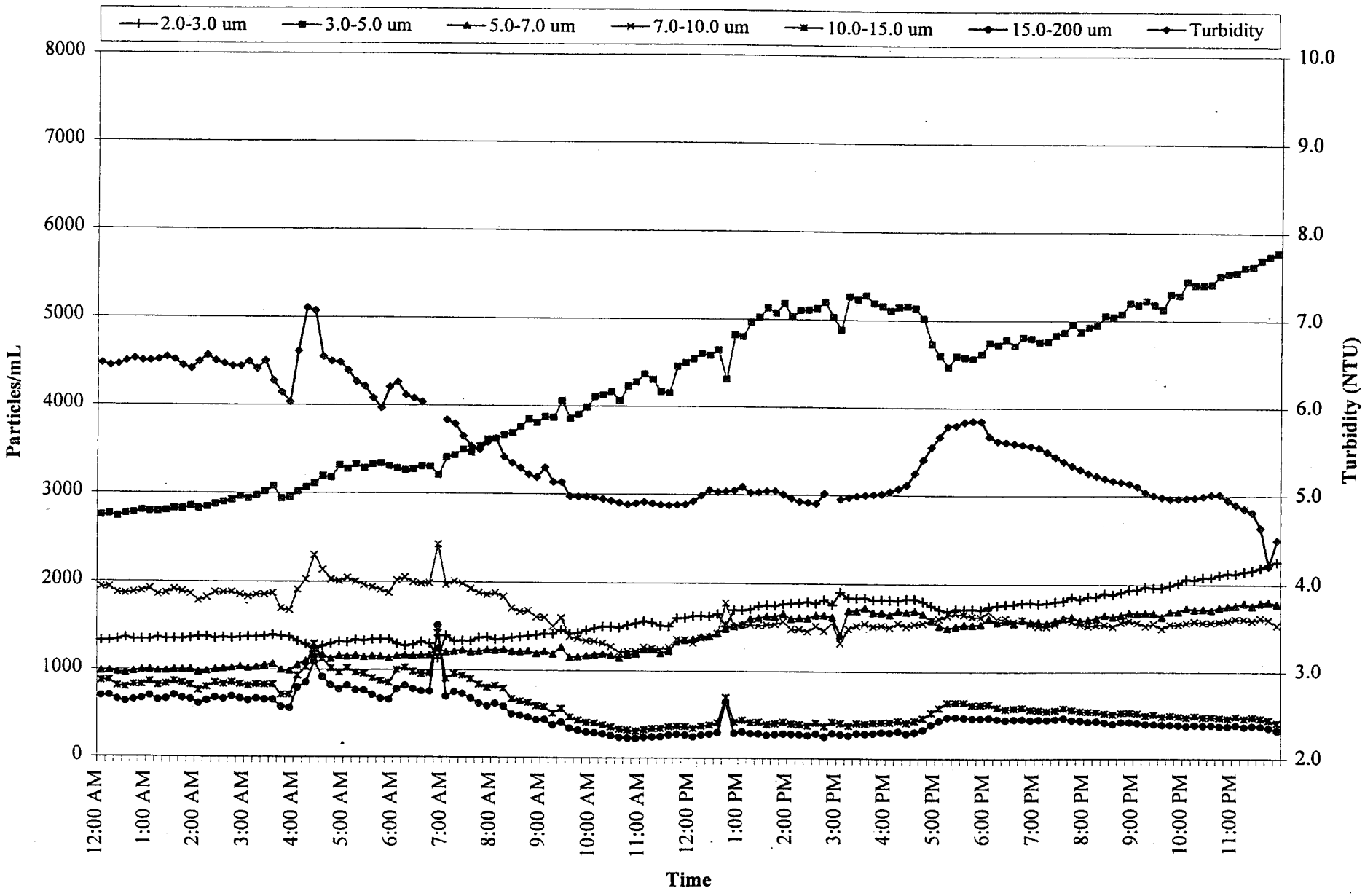

Fig. 3. Particle counts and turbidities of the influent to West Basin pumping station at HTP, 3/13/99.
(a) time series - linear scale

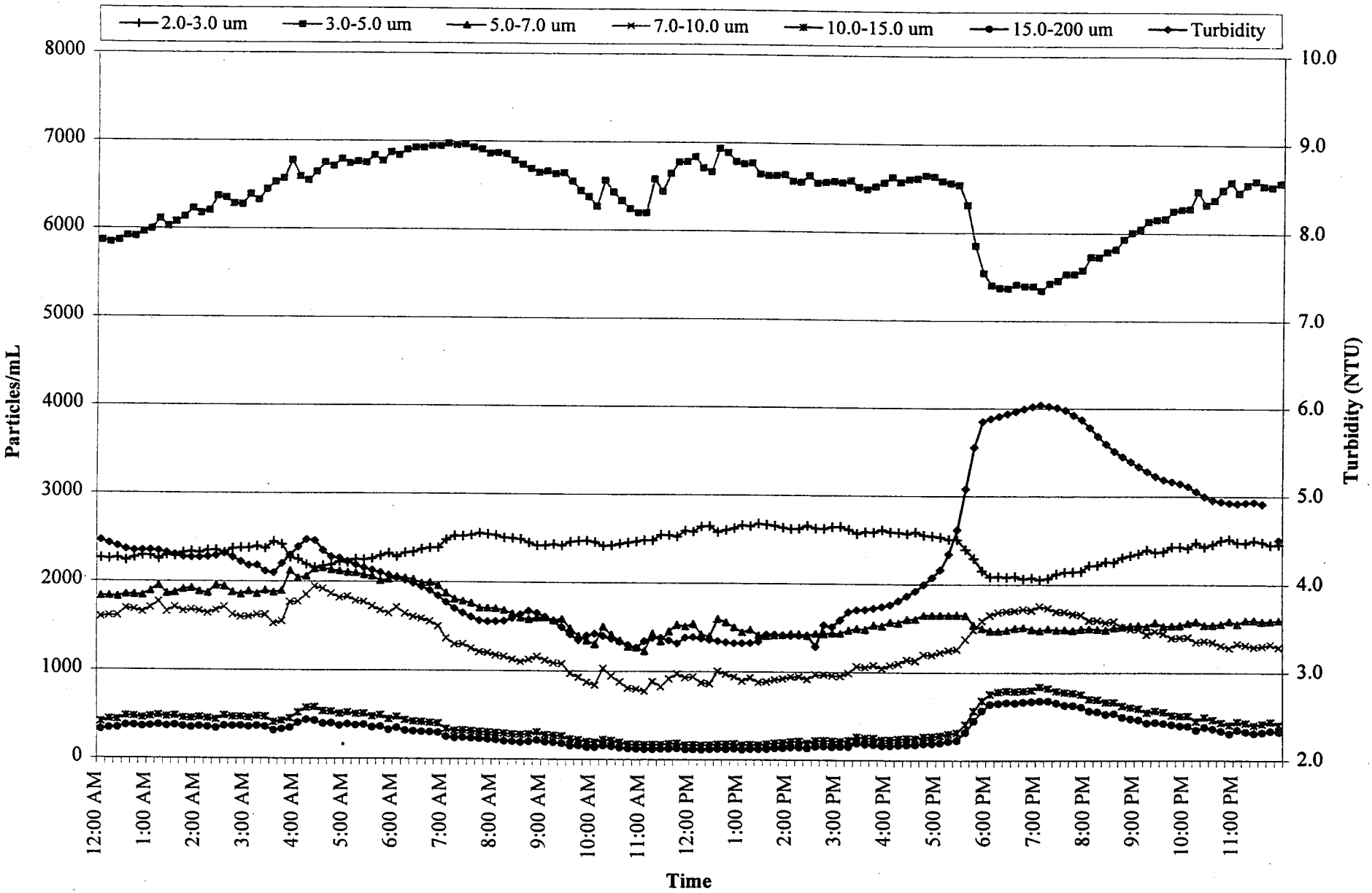

Fig. 4. Particle counts and turbidities of the influent to West Basin pumping station at HTP, 3/14/99.
(a) time series - linear scale

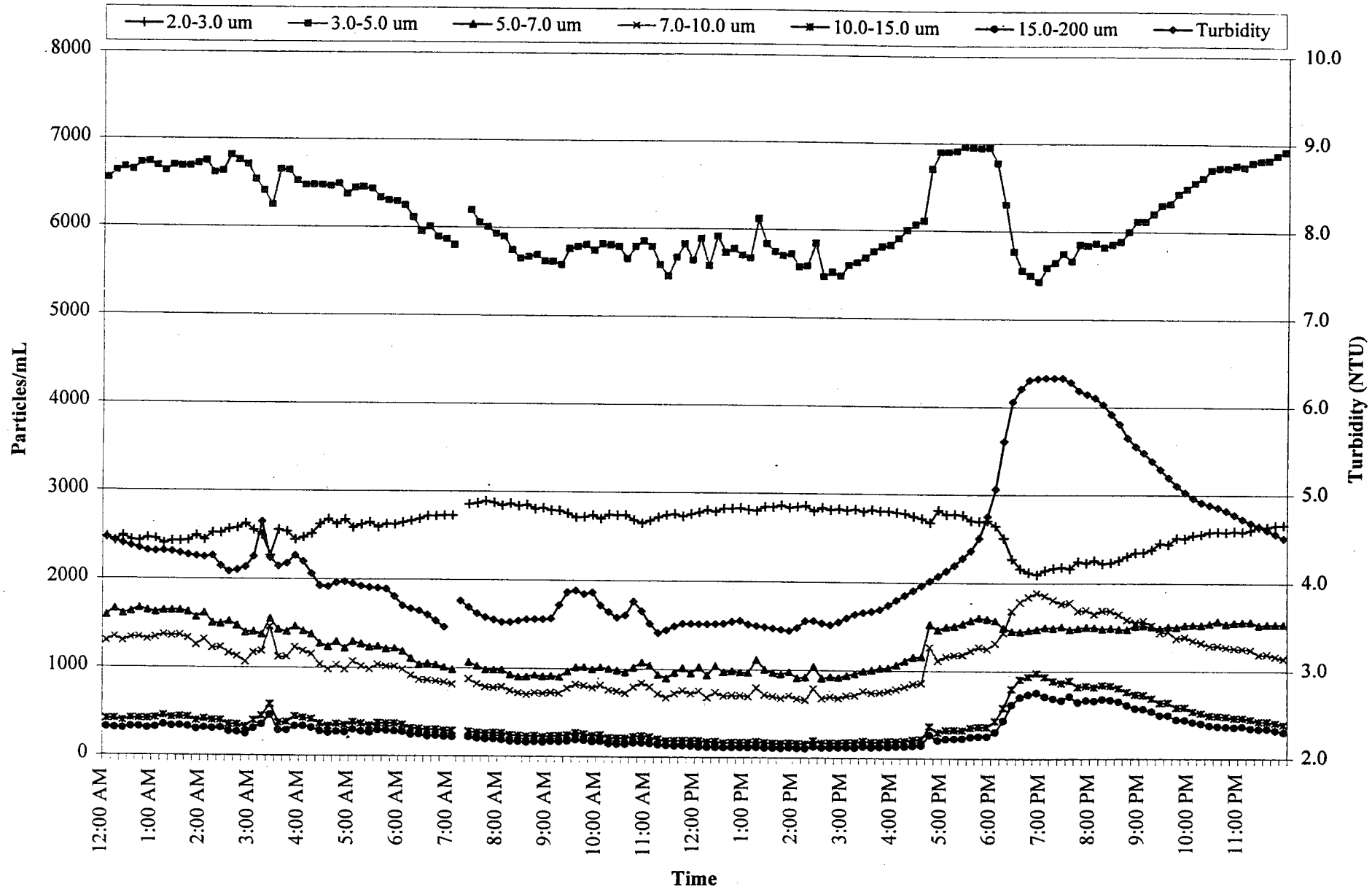

Fig. 5. Particle counts and turbidities of the influent to West Basin pumping station at HTP, 3/15/99.
(a) time series - linear scale

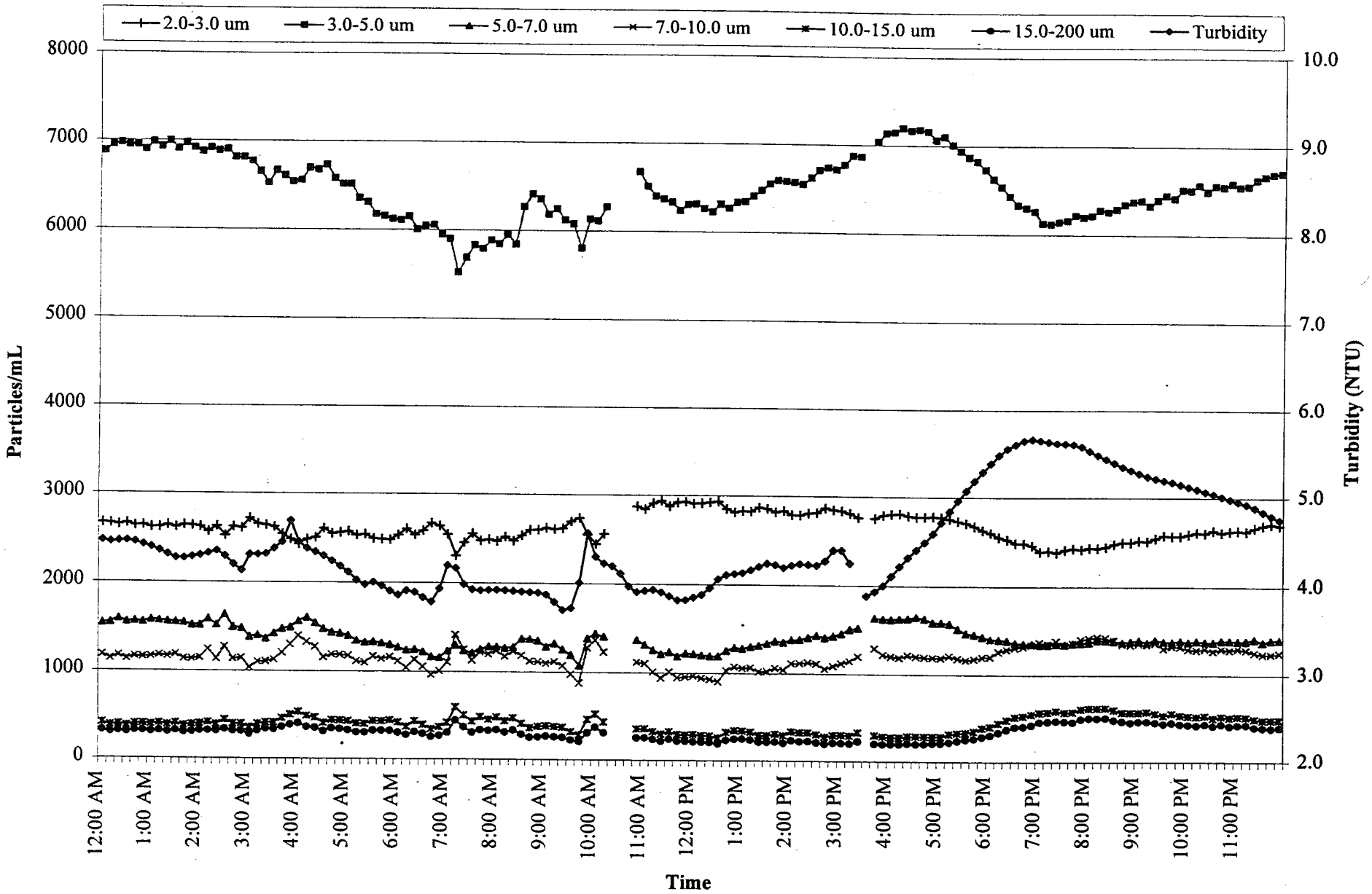

Fig. 6. Particle counts and turbidities of the influent to West Basin pumping station at HTP, 3/16/99.
(a) time series - linear scale

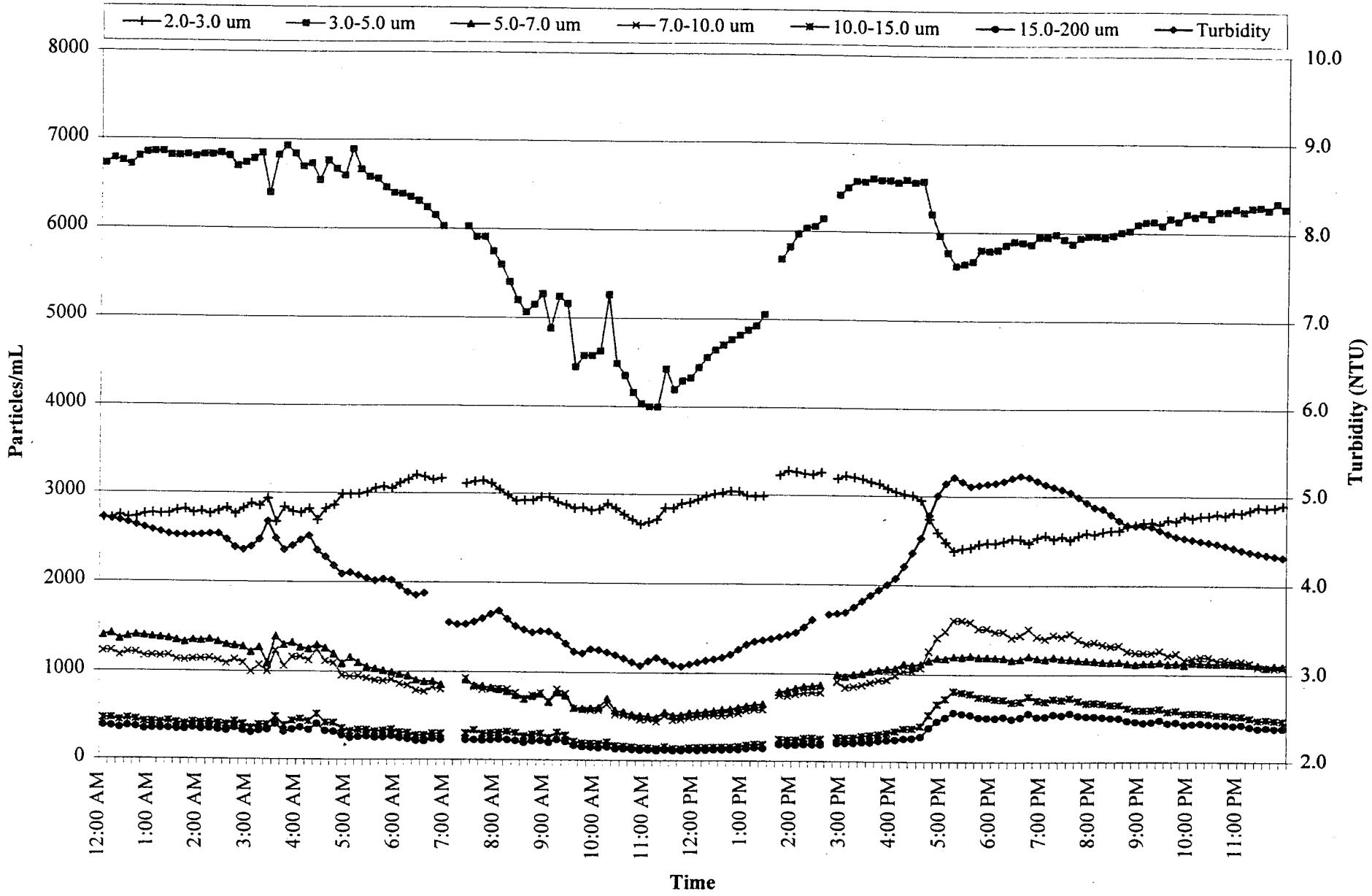

Fig. 7. Particle counts and turbidities of the influent to West Basin pumping station at HTP, 3/17/99.
(a) time series - linear scale

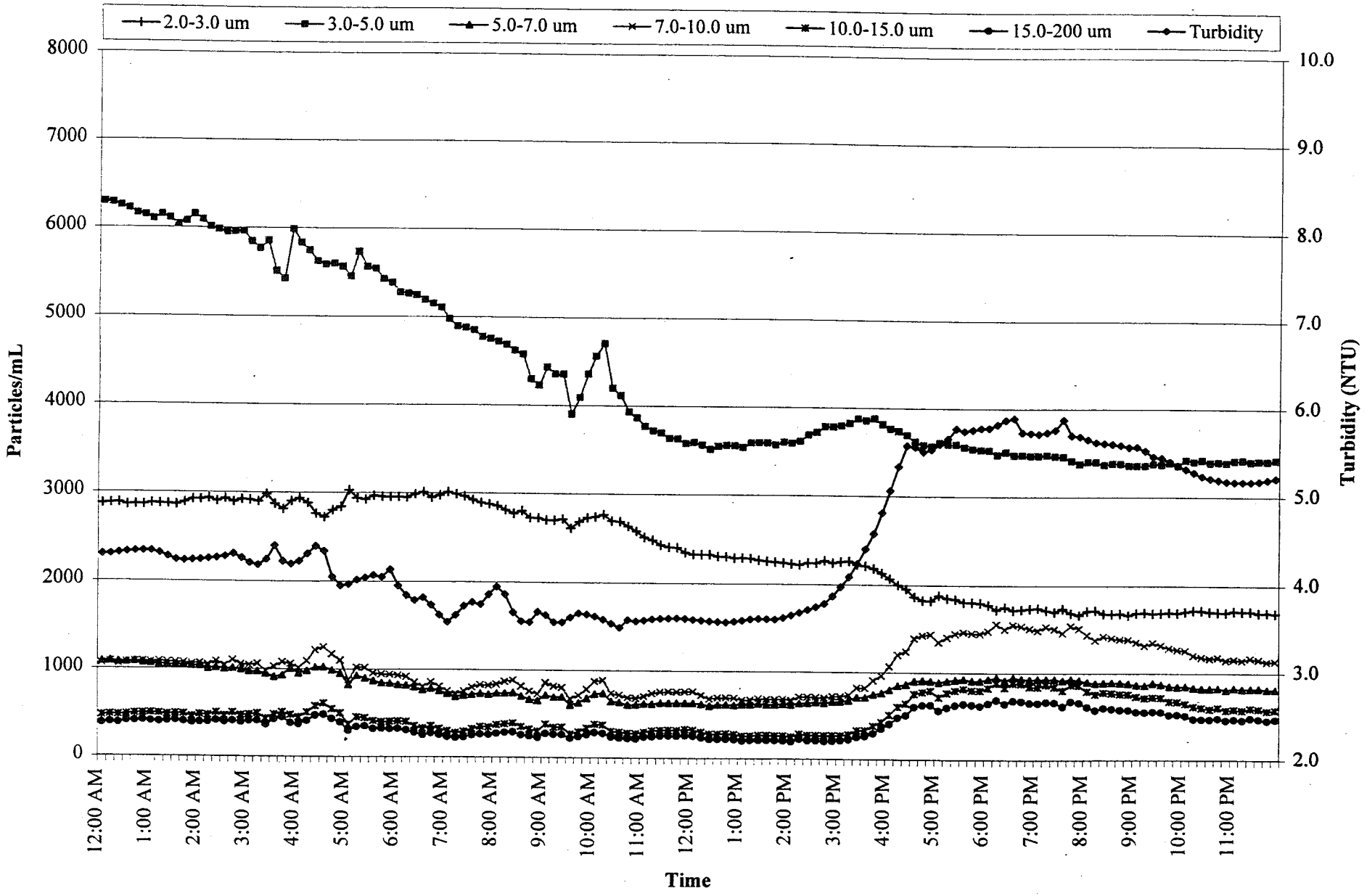

Fig. 8. Particle counts and turbidities of the influent to West Basin pumping station at HTP, 3/18/99.
(a) time series - linear scale

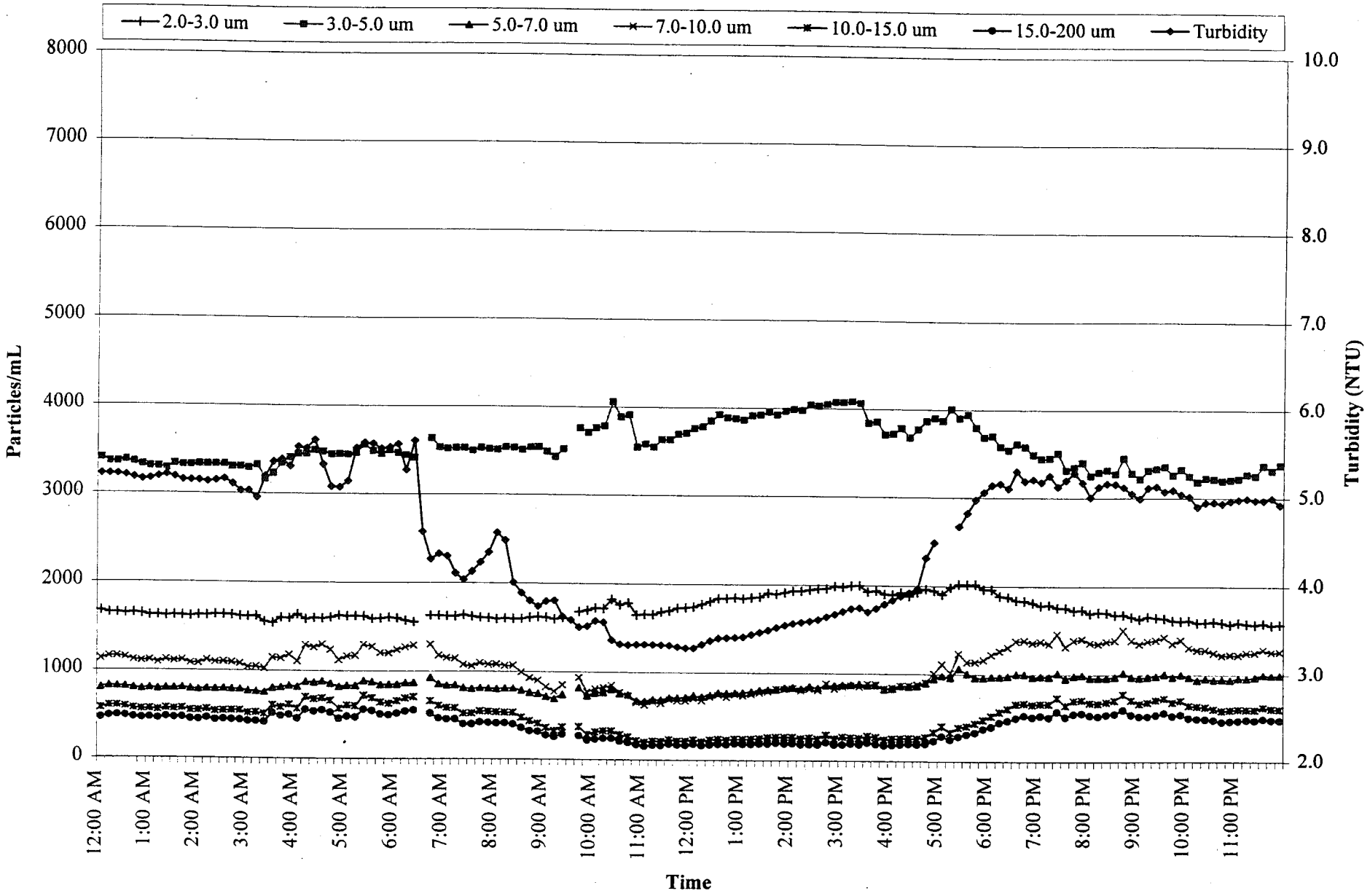

Fig. 9. Particle counts and turbidities of the influent to West Basin pumping station at HTP, 3/19/99.
(a) time series - linear scale

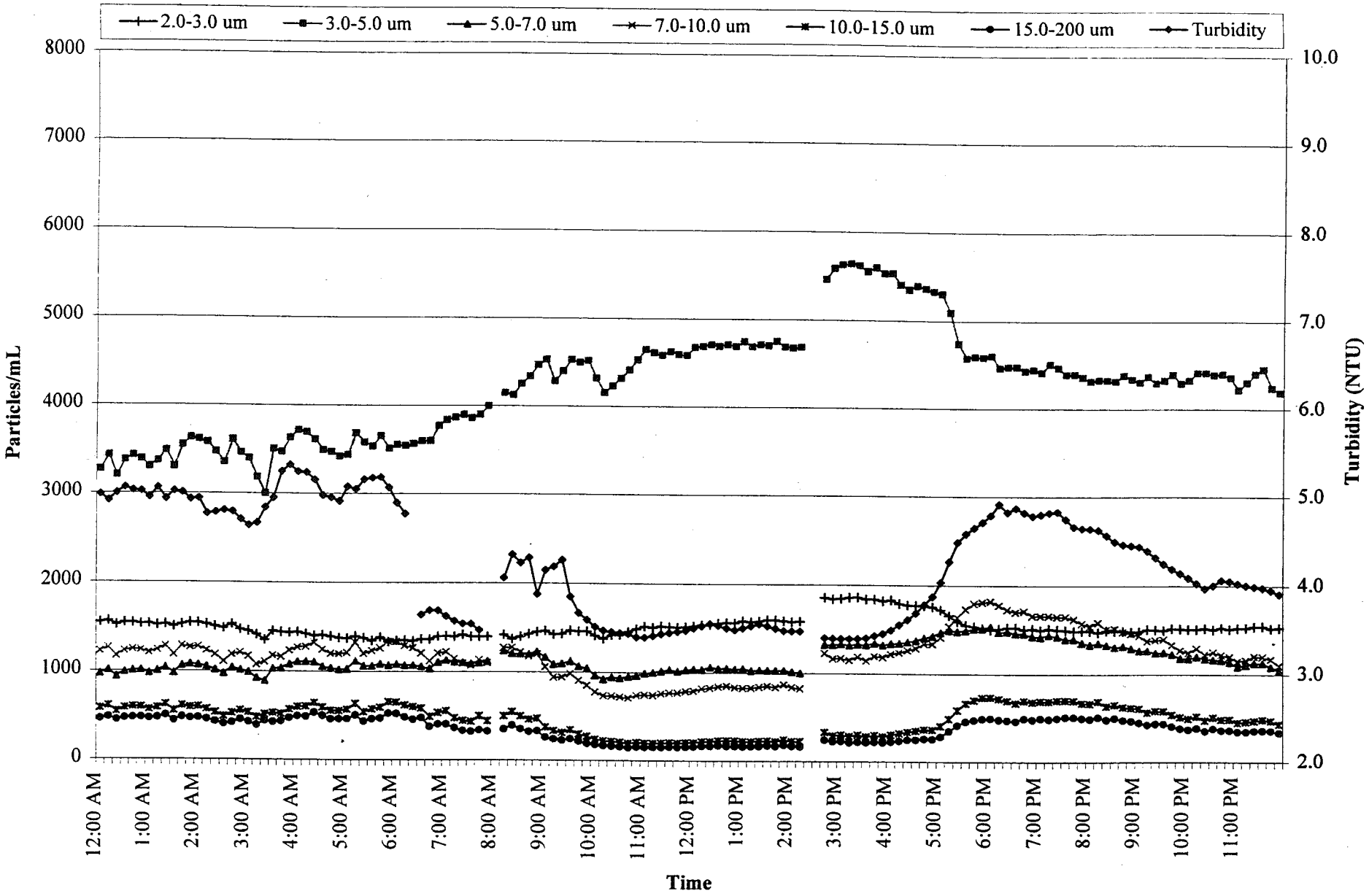

Fig. 10. Particle counts and turbidities of the influent to West Basin pumping station at HTP, 3/20/99.
(a) time series - linear scale

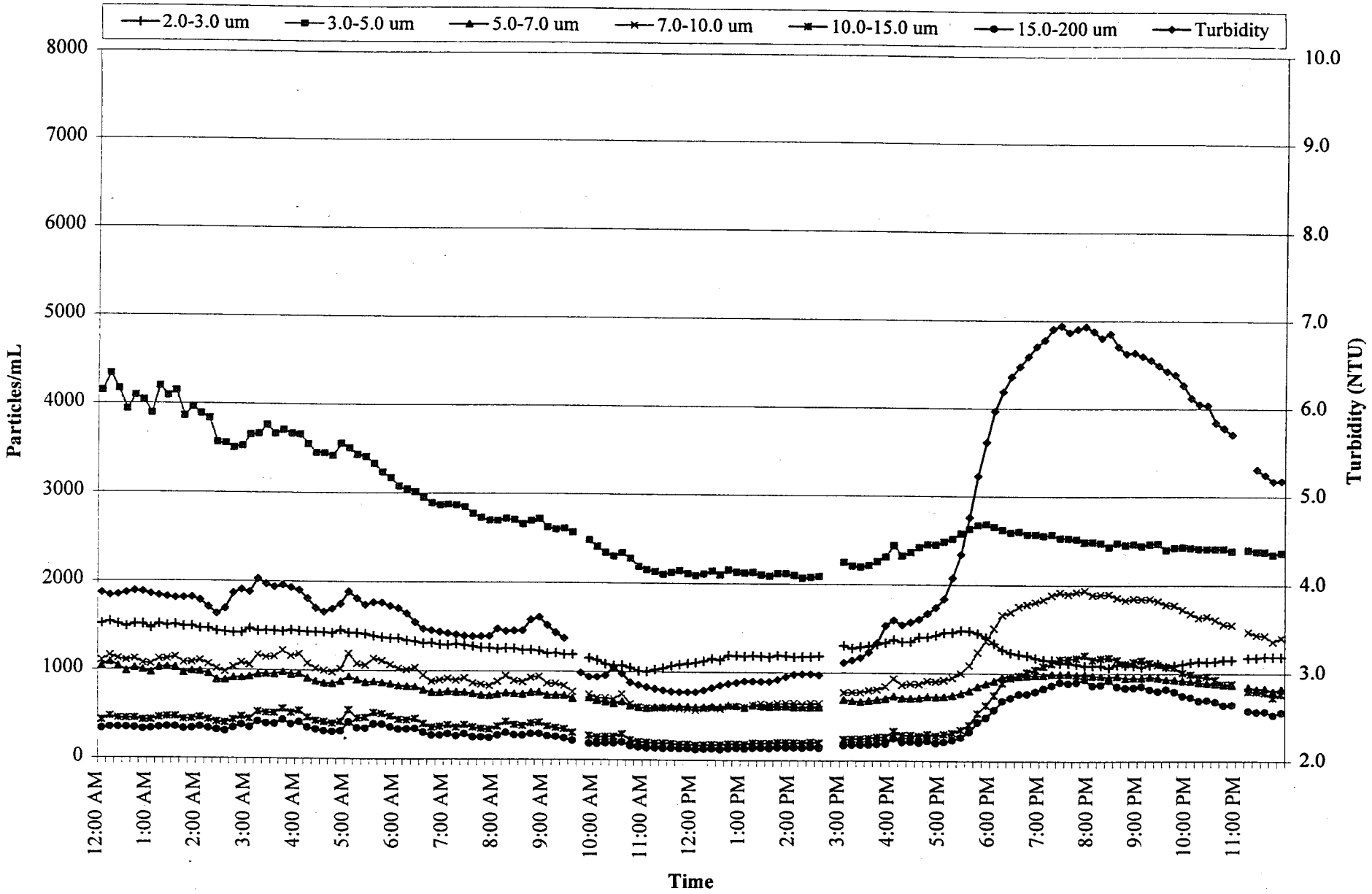

Fig. 11. Particle counts and turbidities of the influent to West Basin pumping station at HTP, 3/21/99.
(a) time series - linear scale

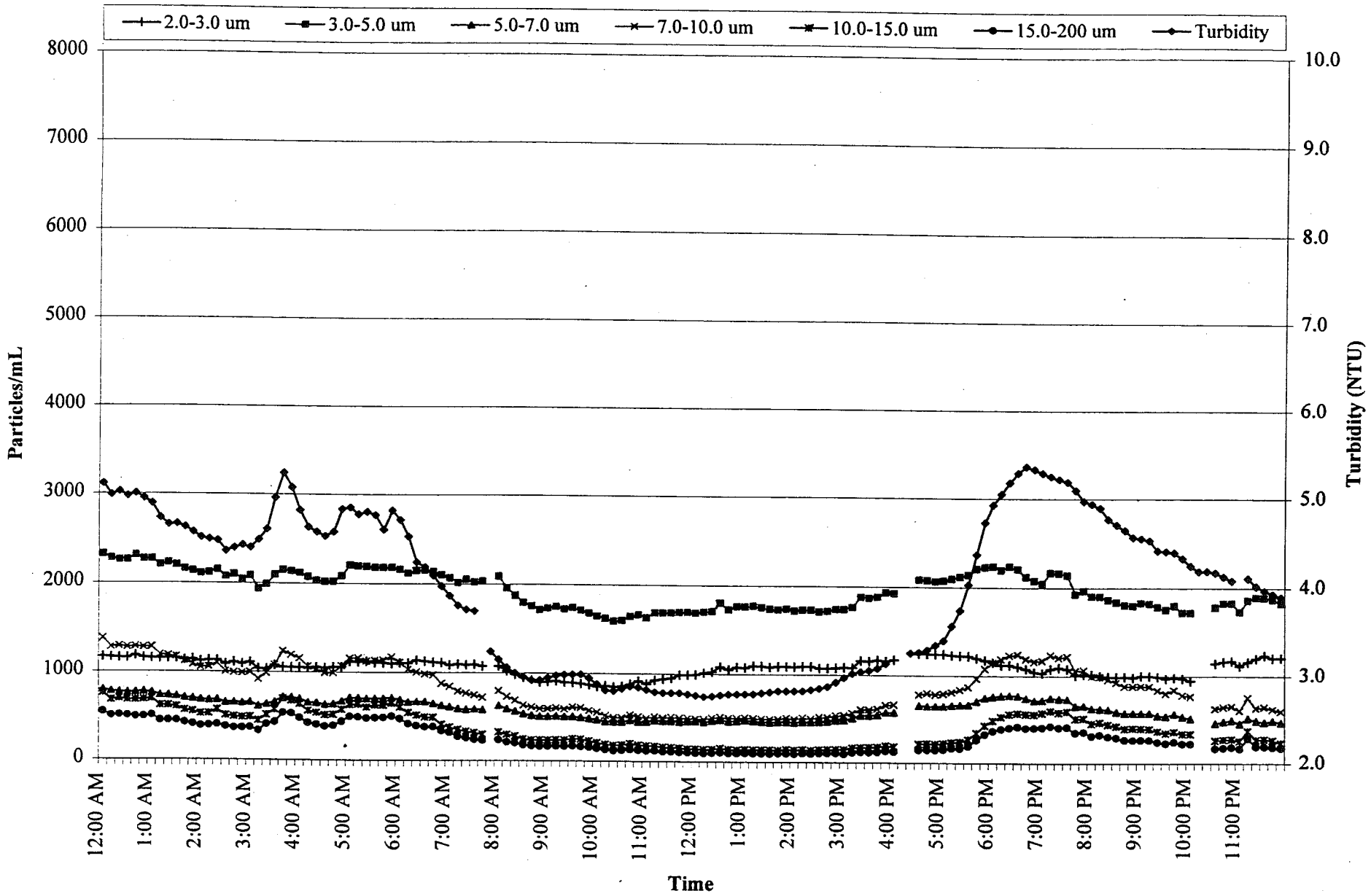

Fig. 12. Particle counts and turbidities of the influent to West Basin pumping station at HTP, 3/22/99.
(a) time series - linear scale

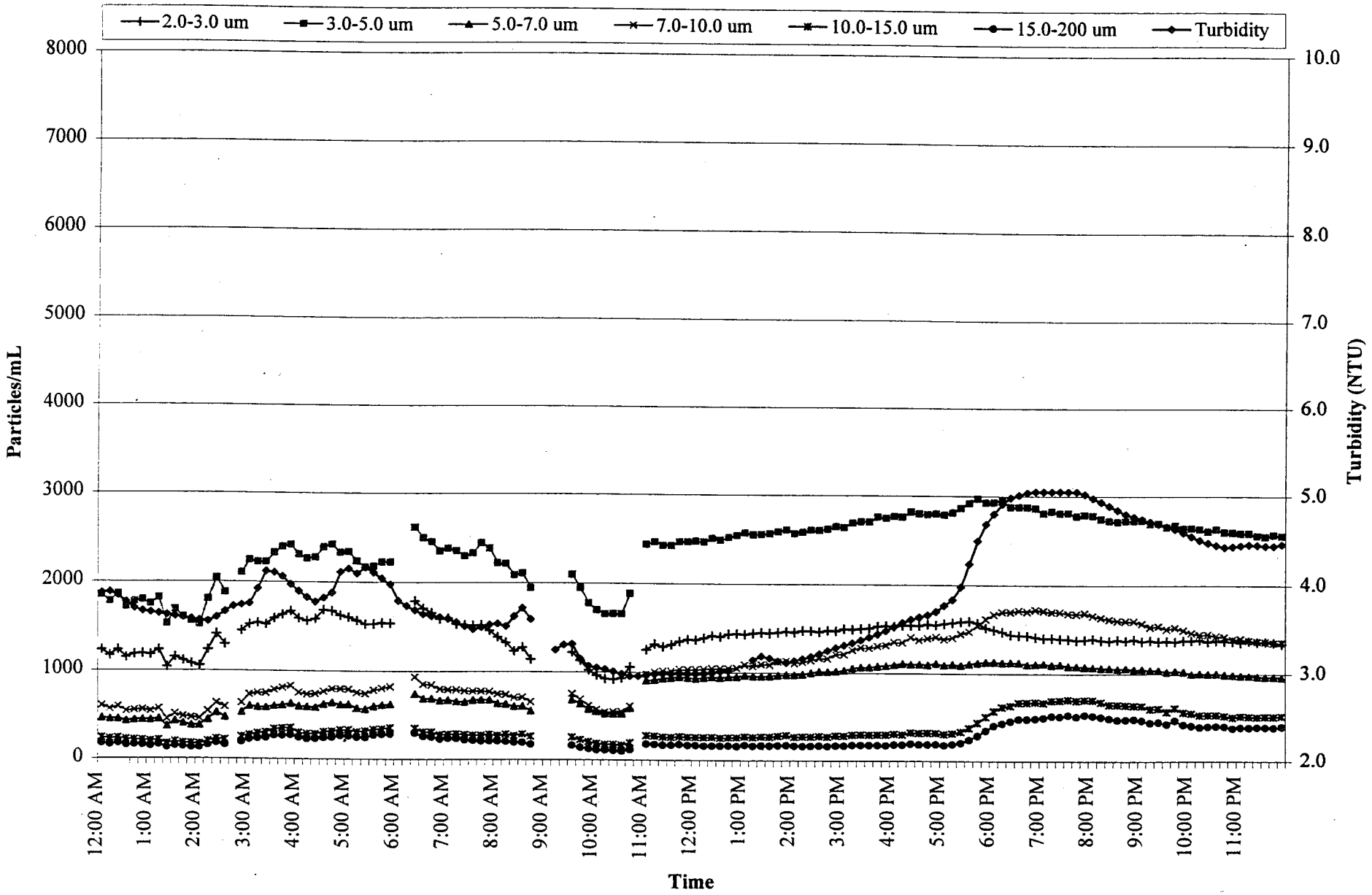

Fig. 13. Particle counts and turbidities of the influent to West Basin pumping station at HTP, 3/23/99.
(a) time series - linear scale

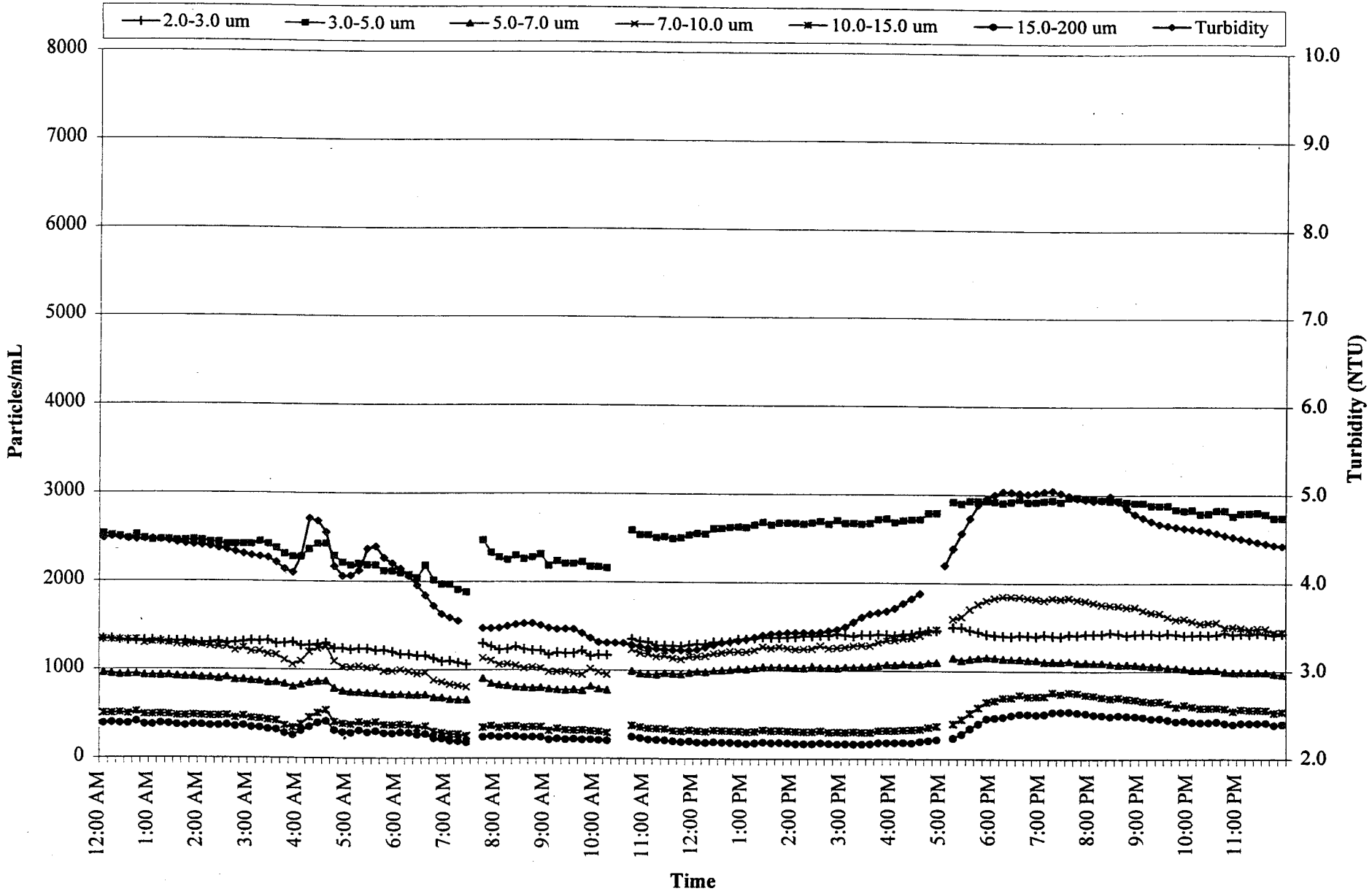

Fig. 14. Particle counts and turbidities of the influent to West Basin pumping station at HTP, 3/24/99.
(a) time series - linear scale

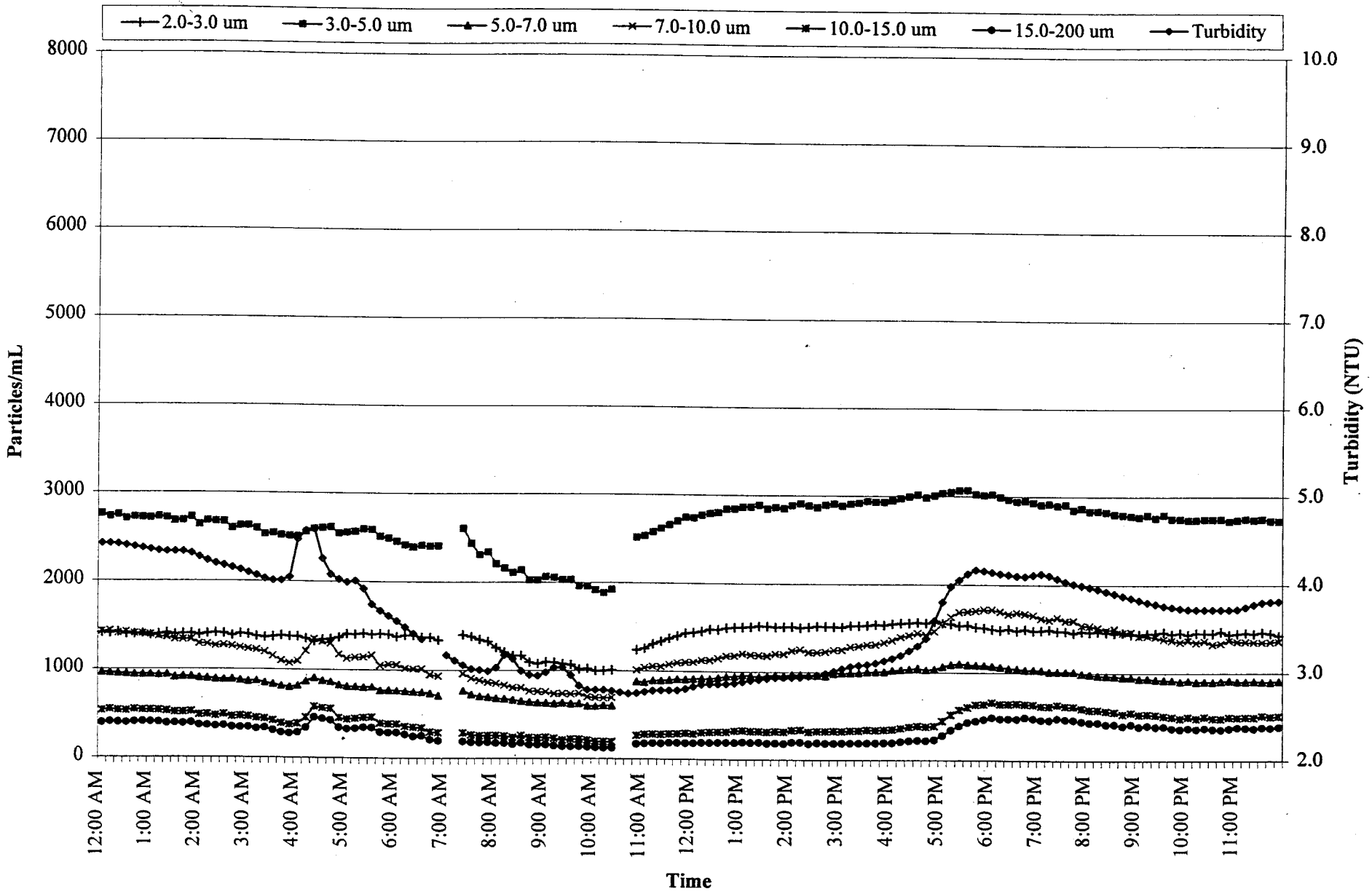

Fig. 1. Continued.

(b) time series - log scale

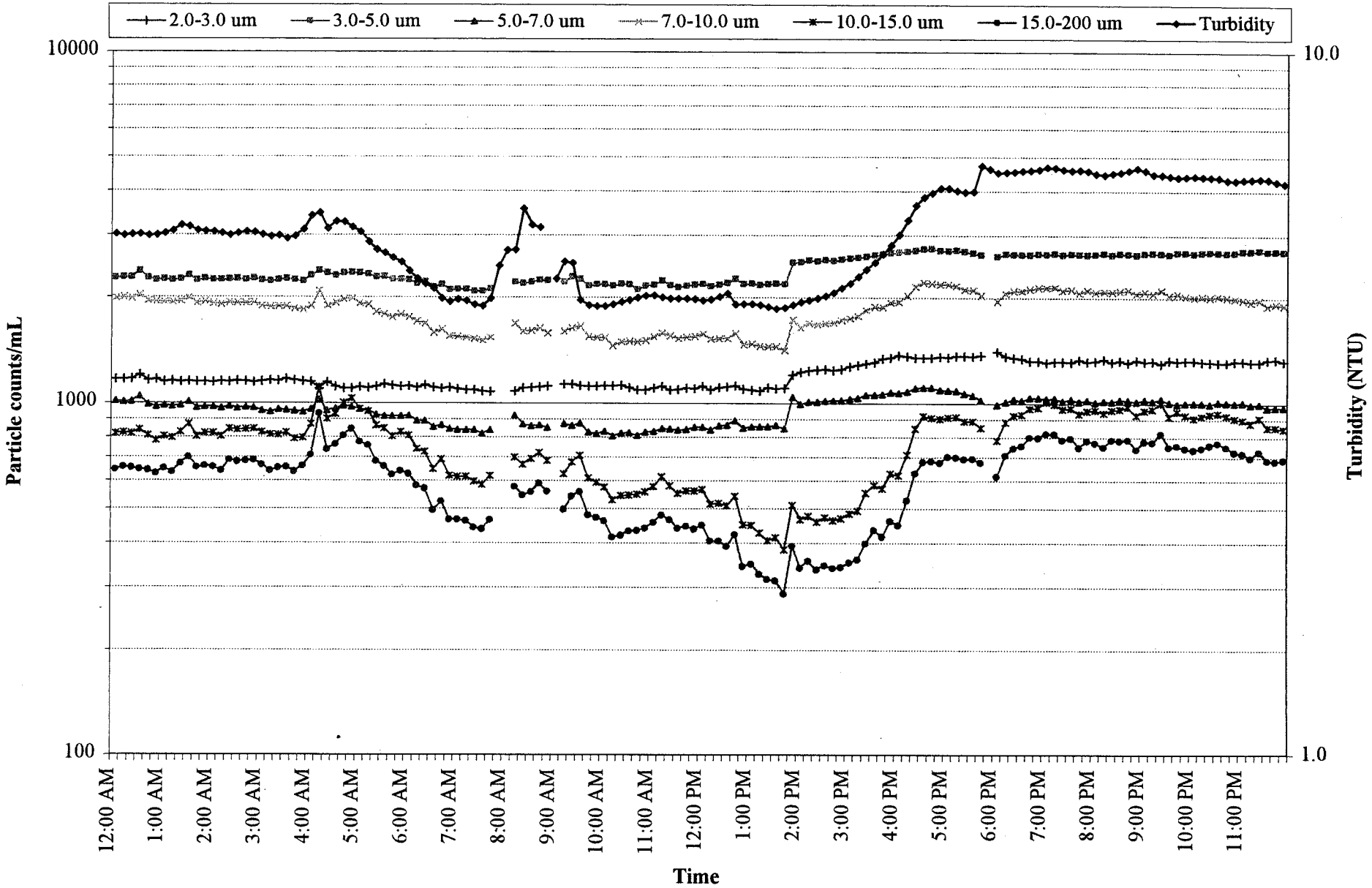

Fig. 2. Continued.

(b) time series - log scale

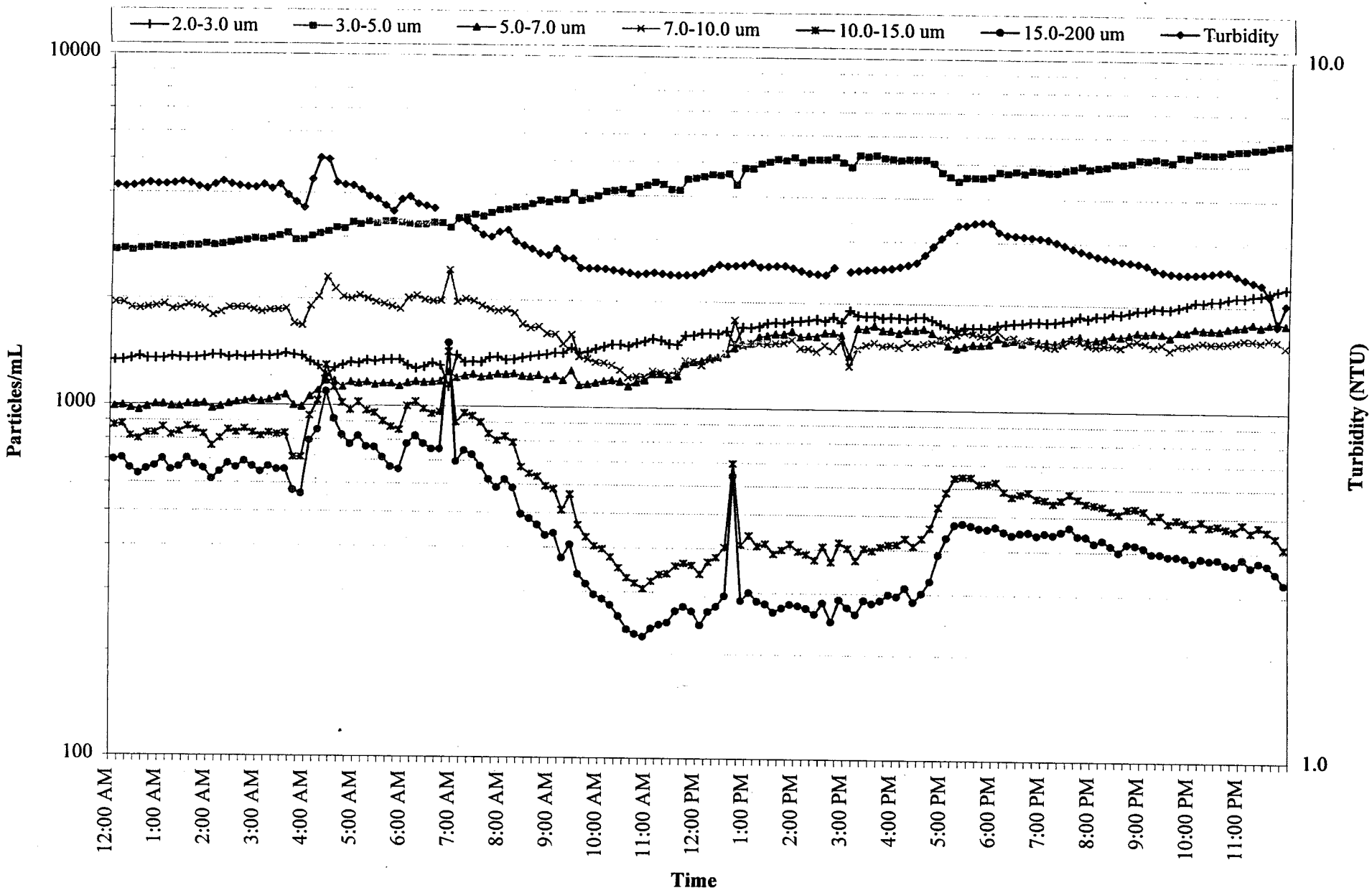

Fig. 3. Continued.

(b) time series - log scale

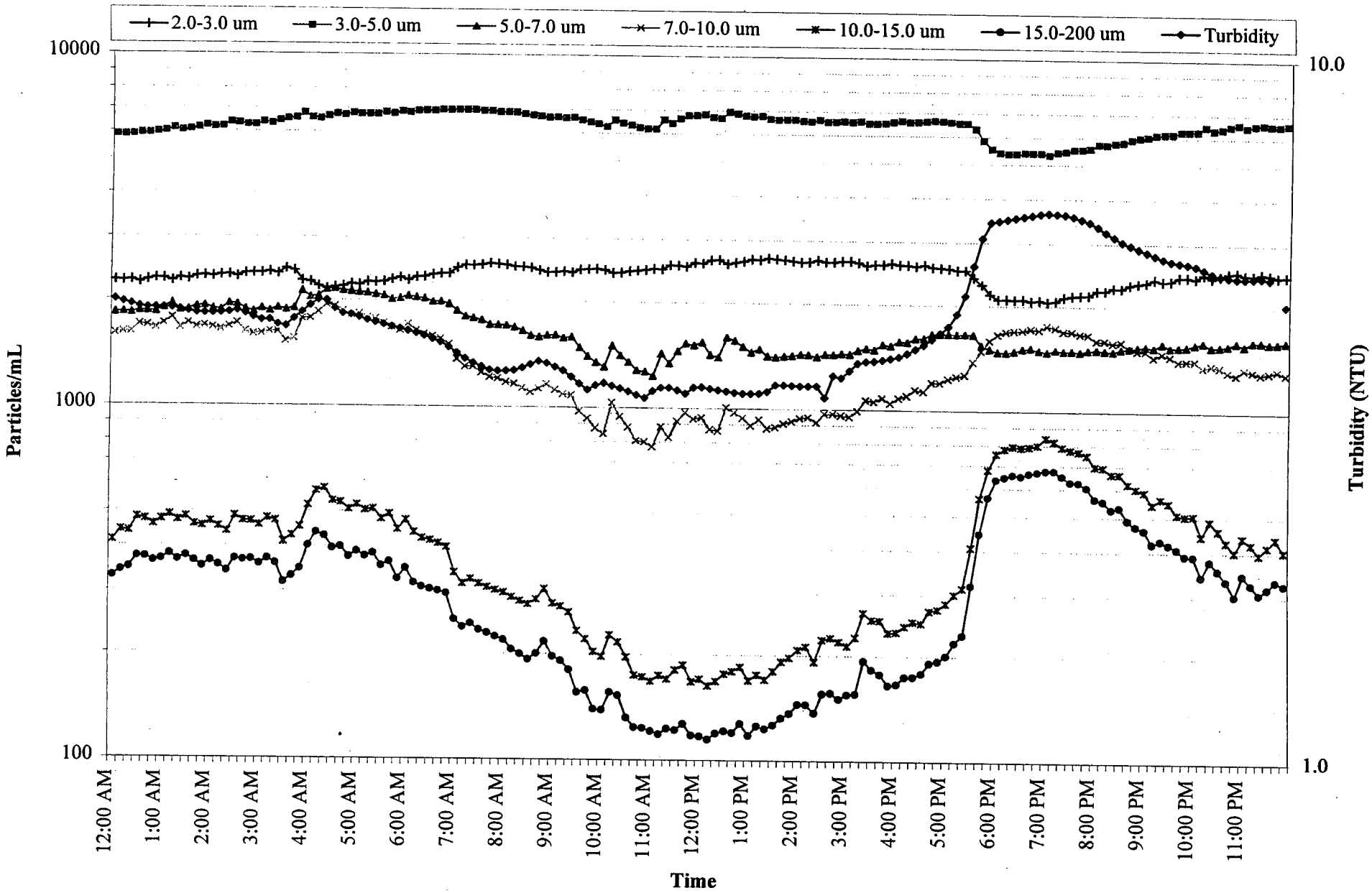

Fig. 4. Continued.

(b) time series - log scale

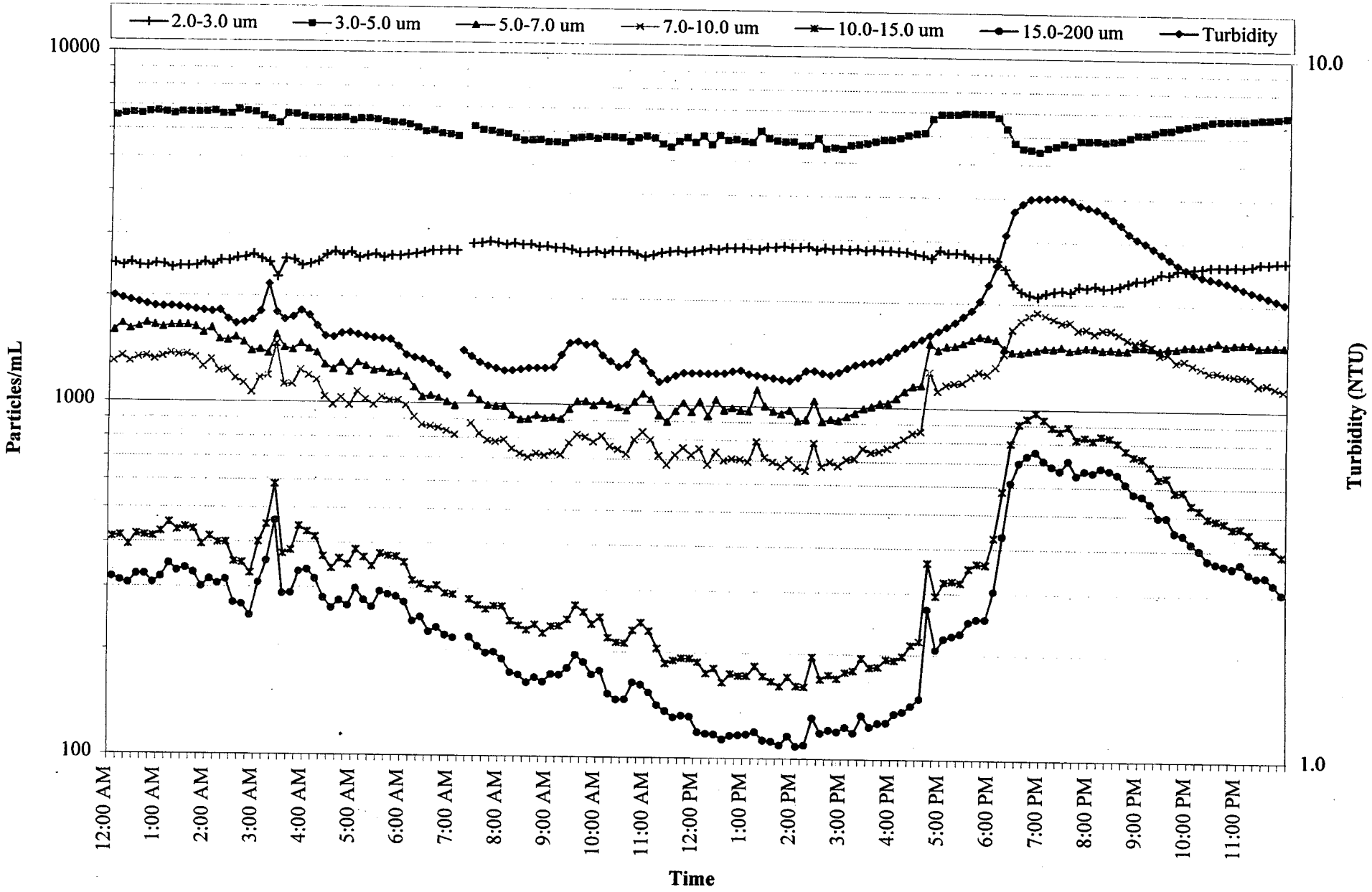

Fig. 5. Continued.

(b) time series - log scale

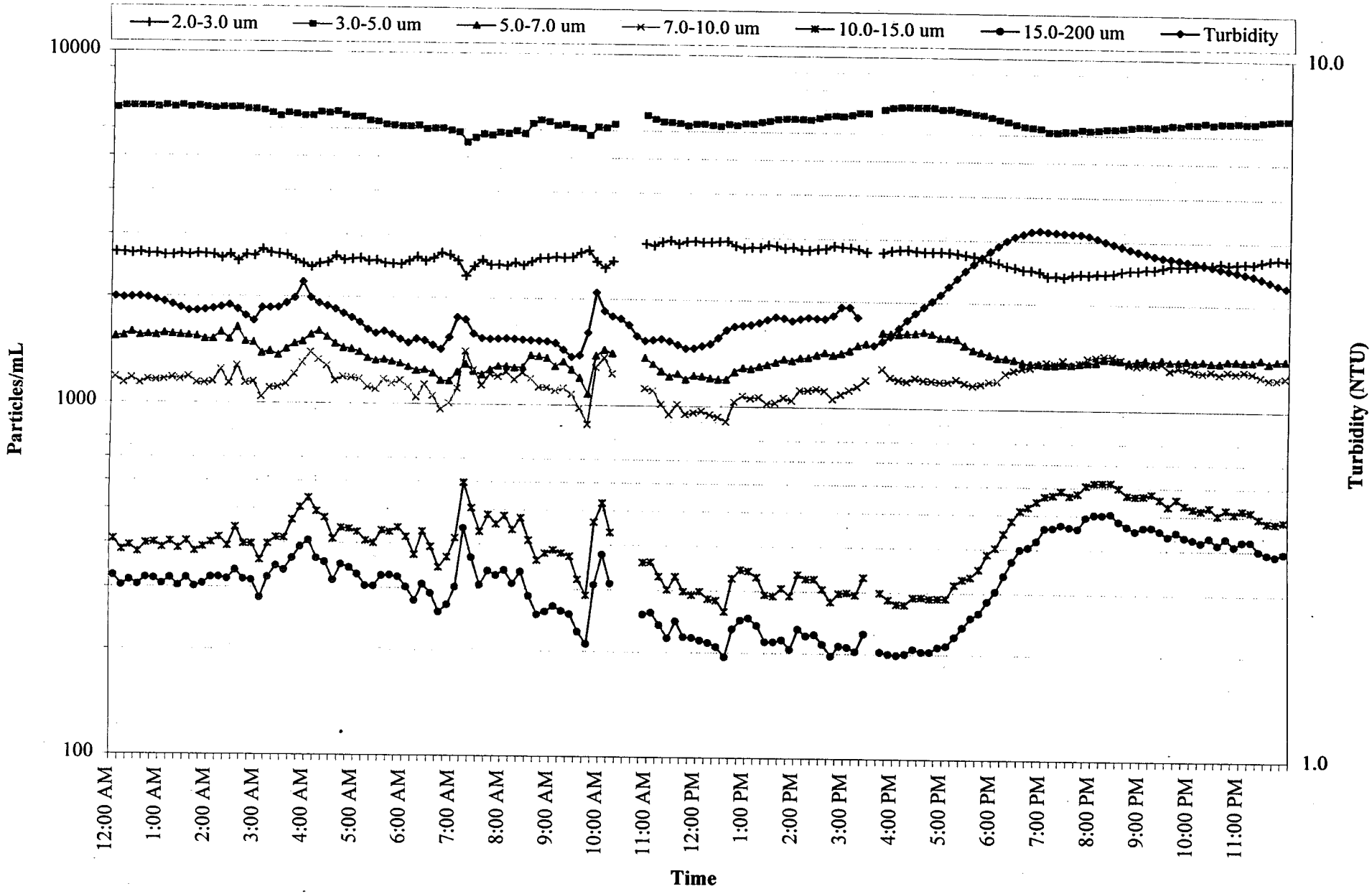

Fig. 6. Continued.

(b) time series - log scale

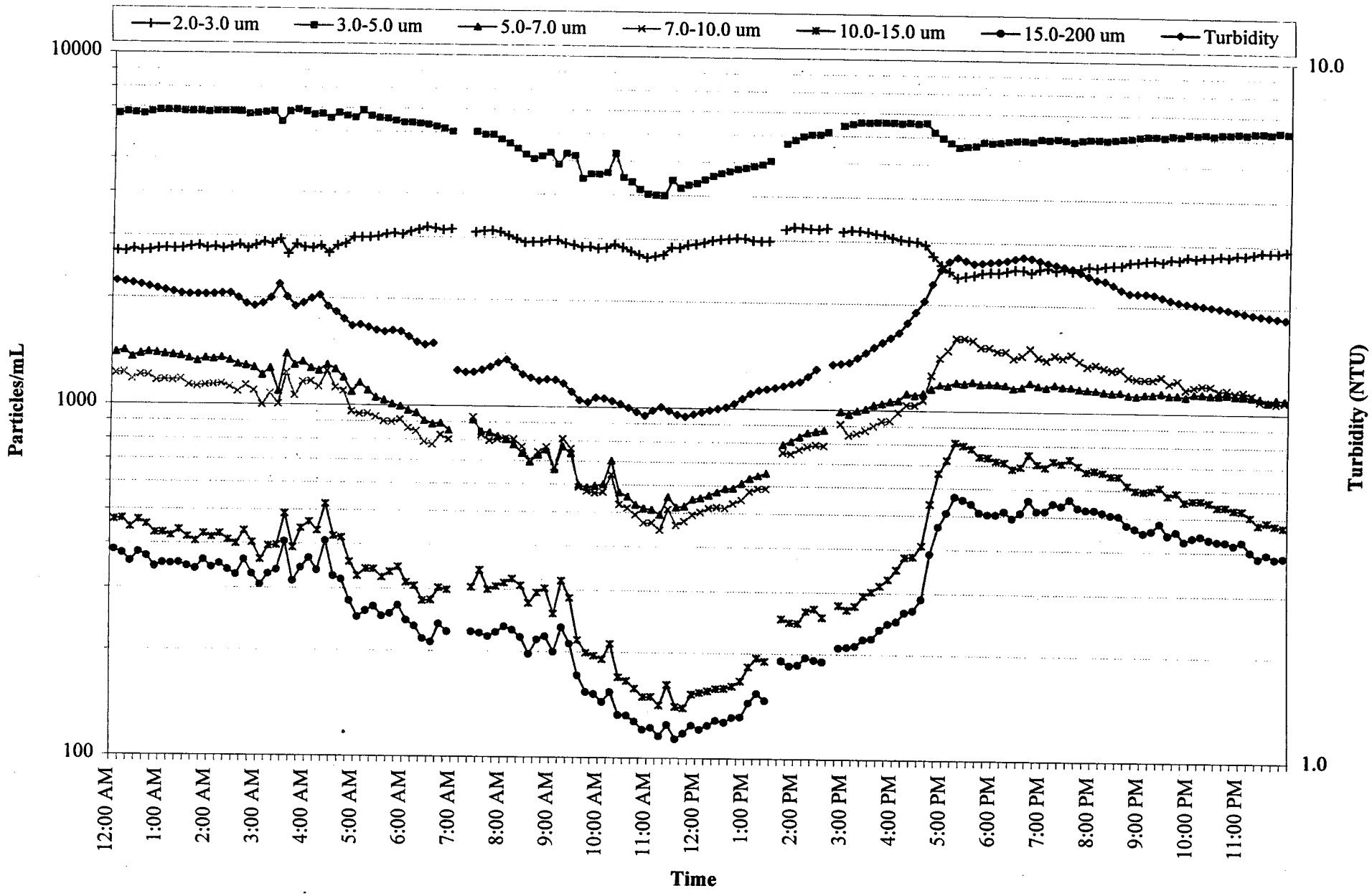

Fig. 7. Continued.

(b) time series - log scale

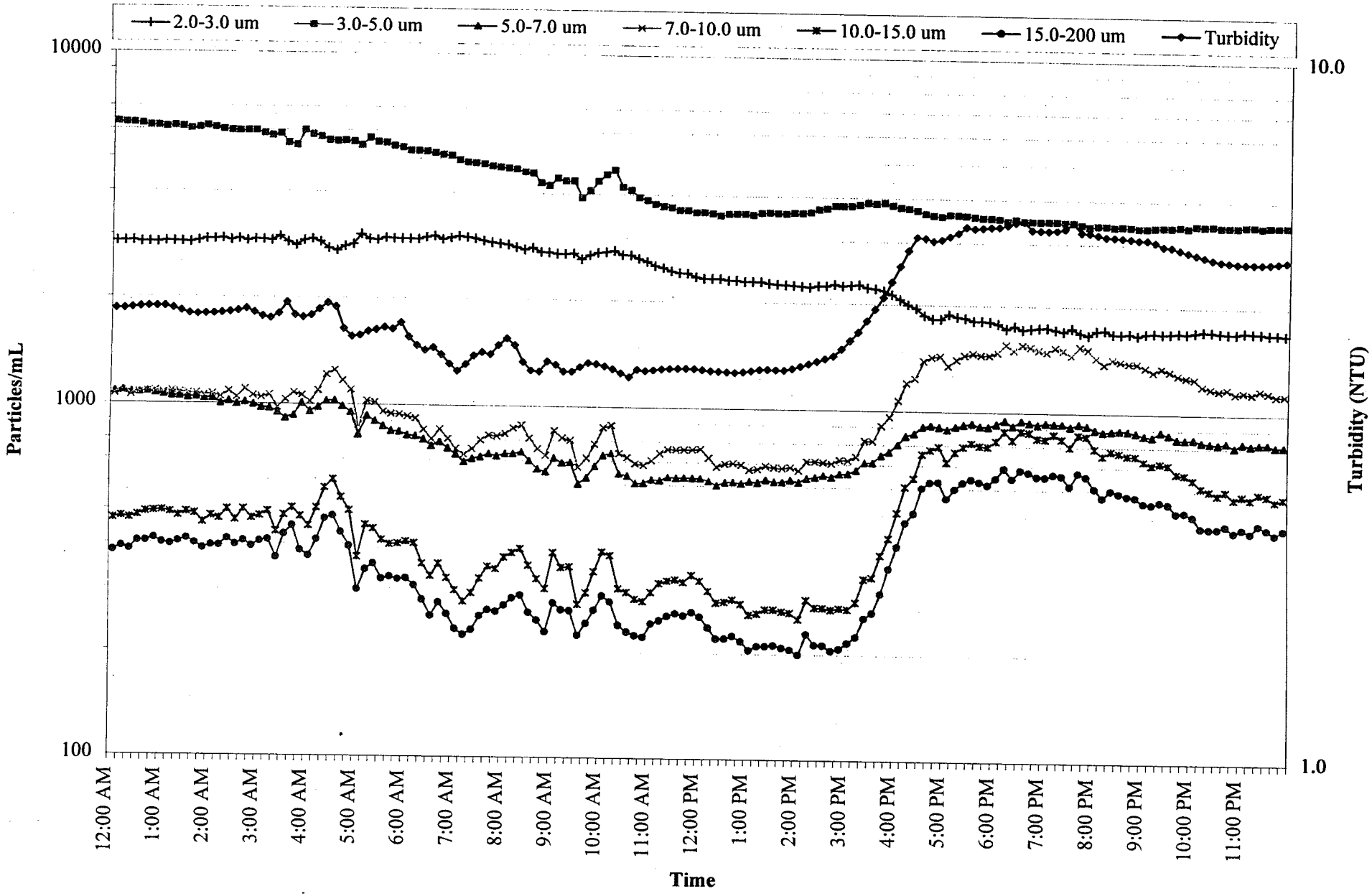

Fig. 8. Continued.

(b) time series - log scale

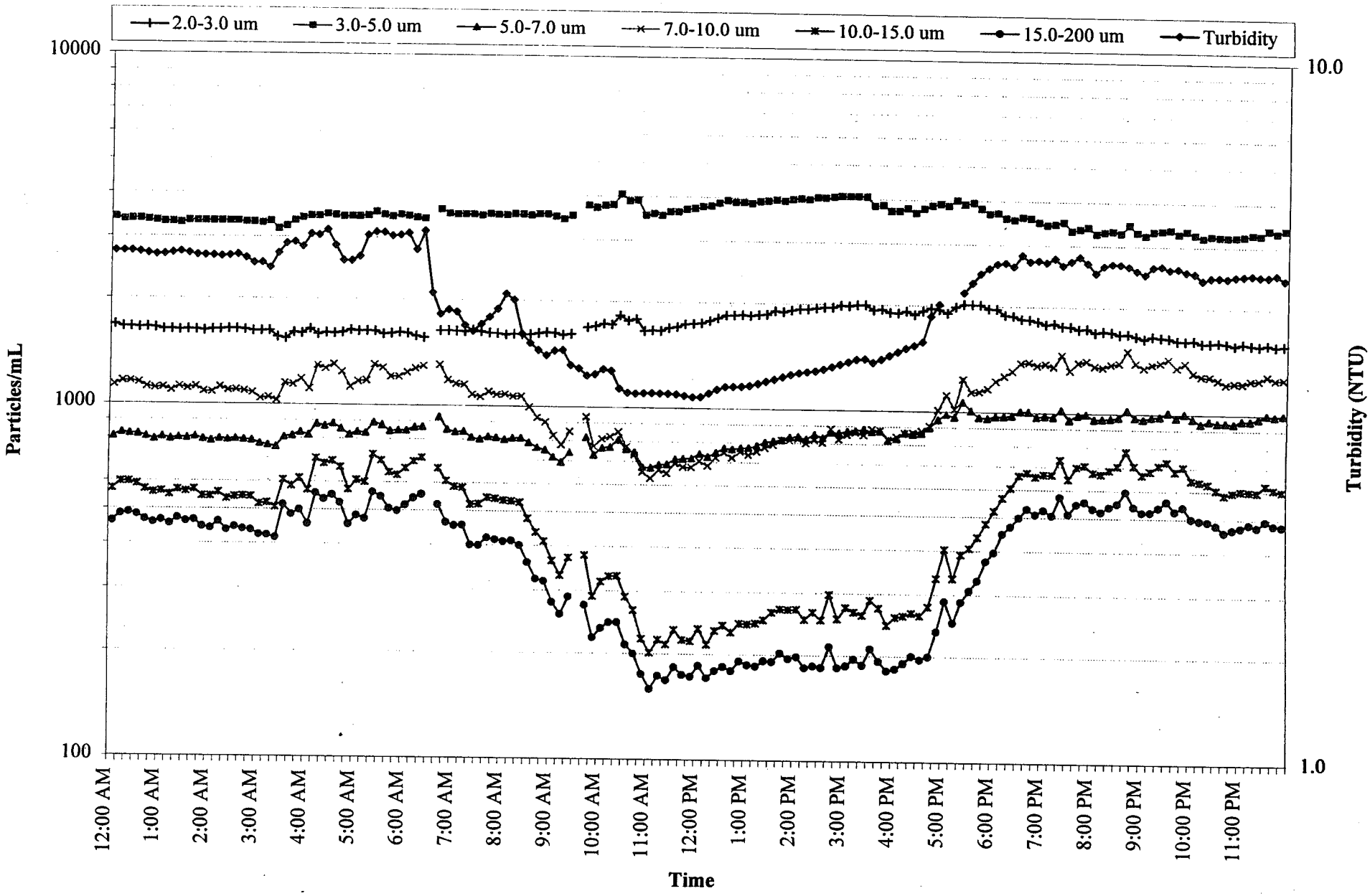

Fig. 9. Continued.

(b) time series - log scale

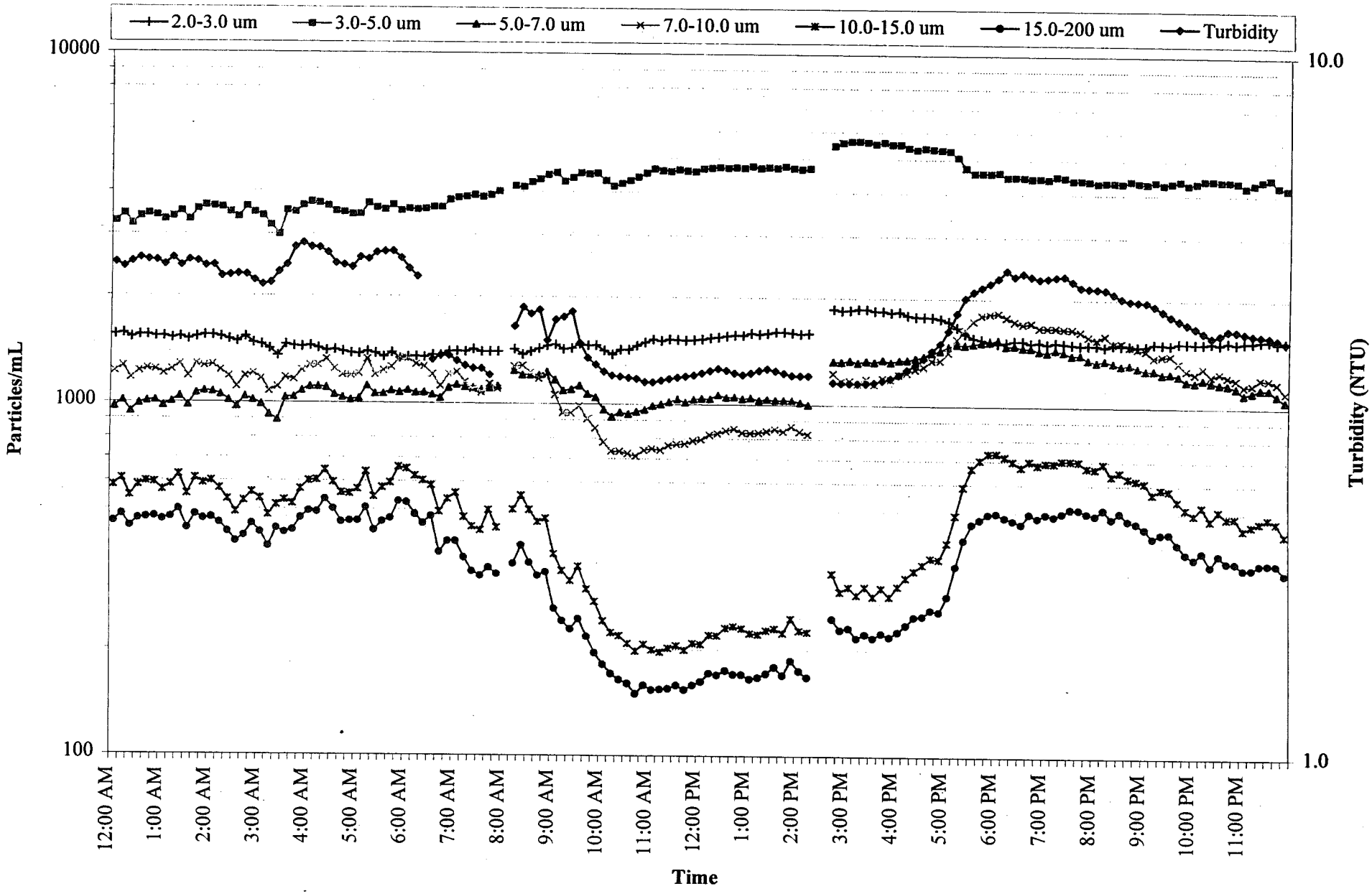

Fig. 10. Continued.

(b) time series - log scale

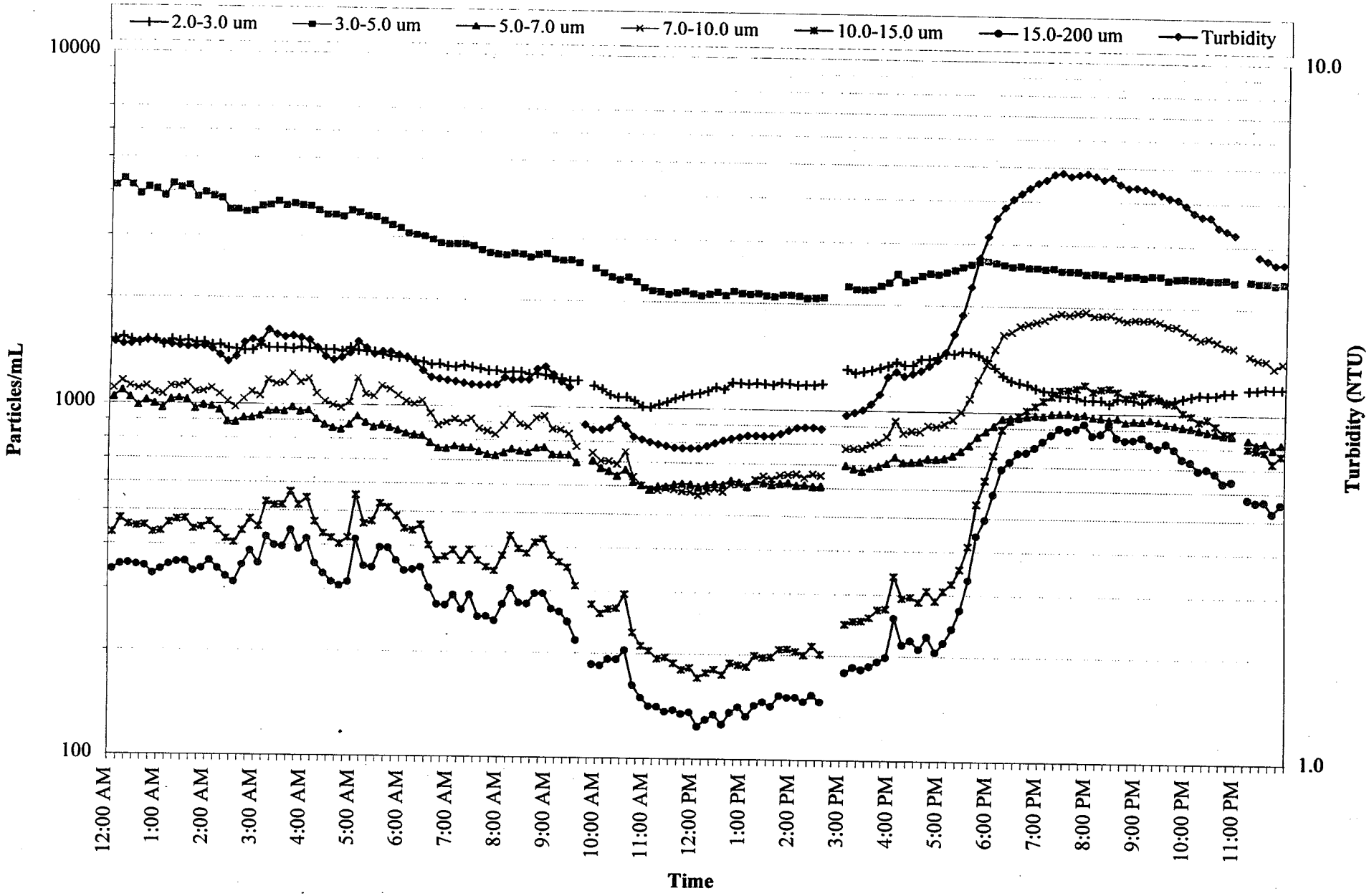

Fig. 11. Continued.

(b) time series - log scale

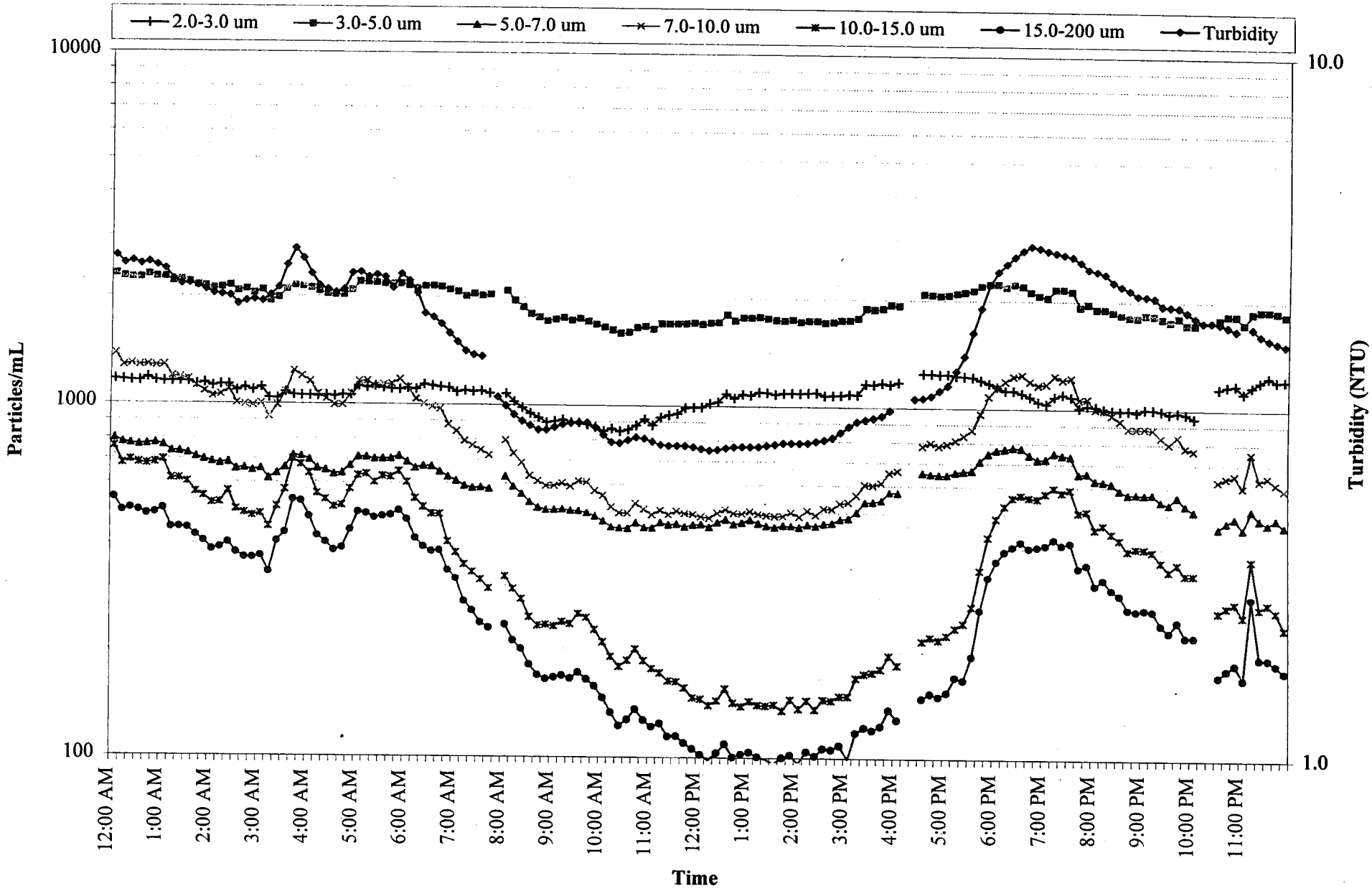

Fig. 12. Continued.

(b) time series - log scale

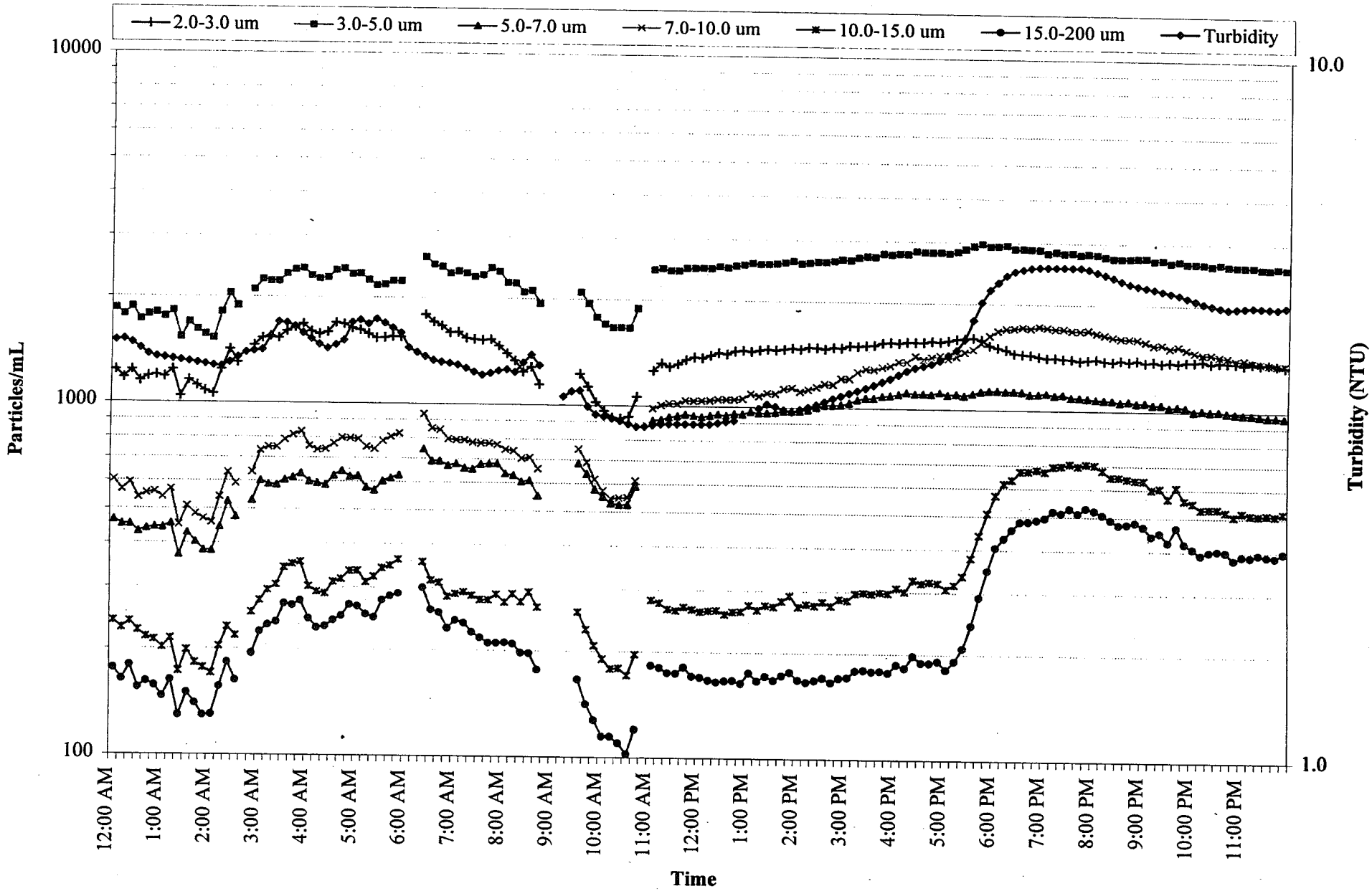

Fig. 13. Continued.

(b) time series - log scale

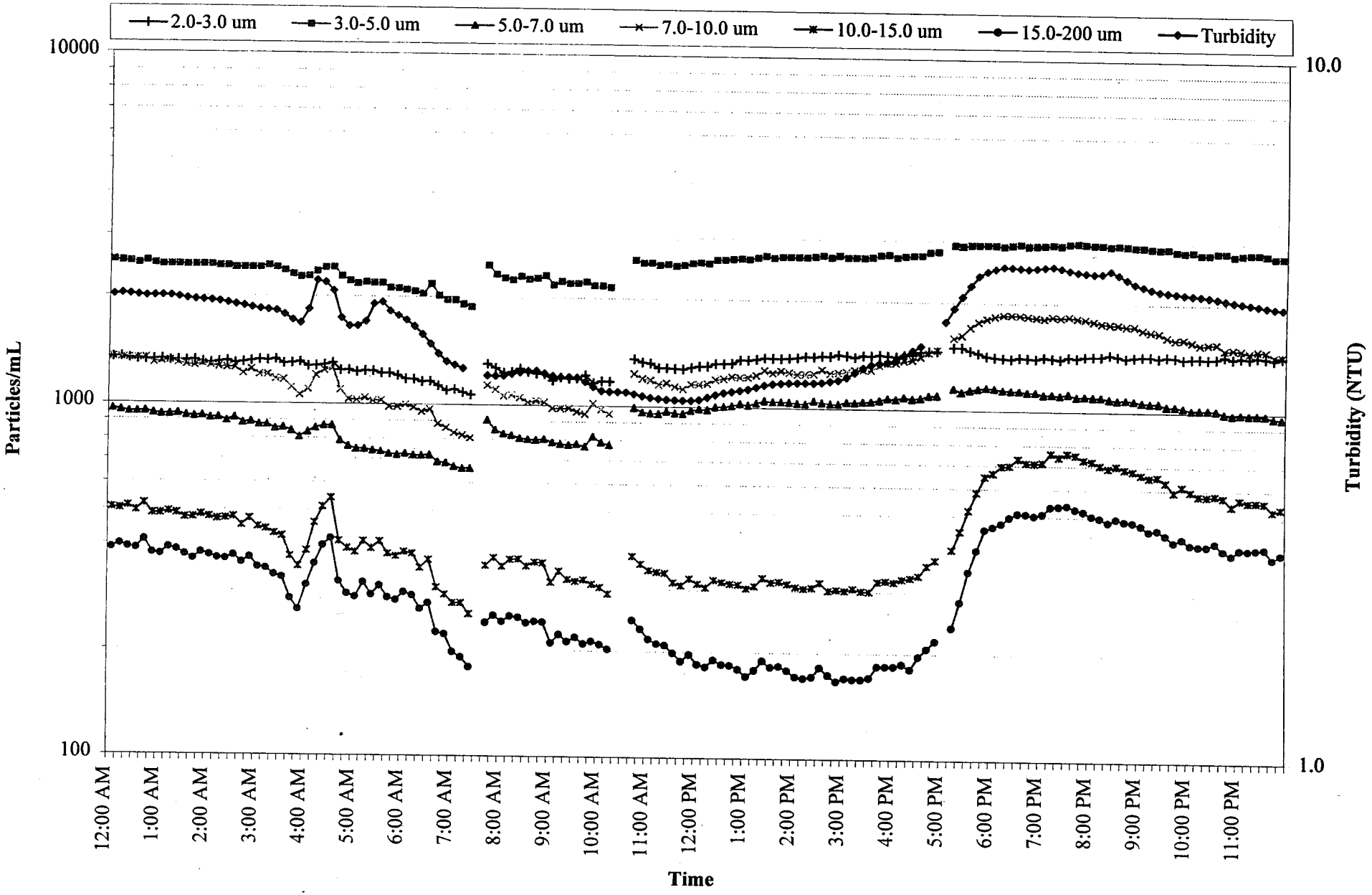

Fig. 14. Continued.

(b) time series - log scale

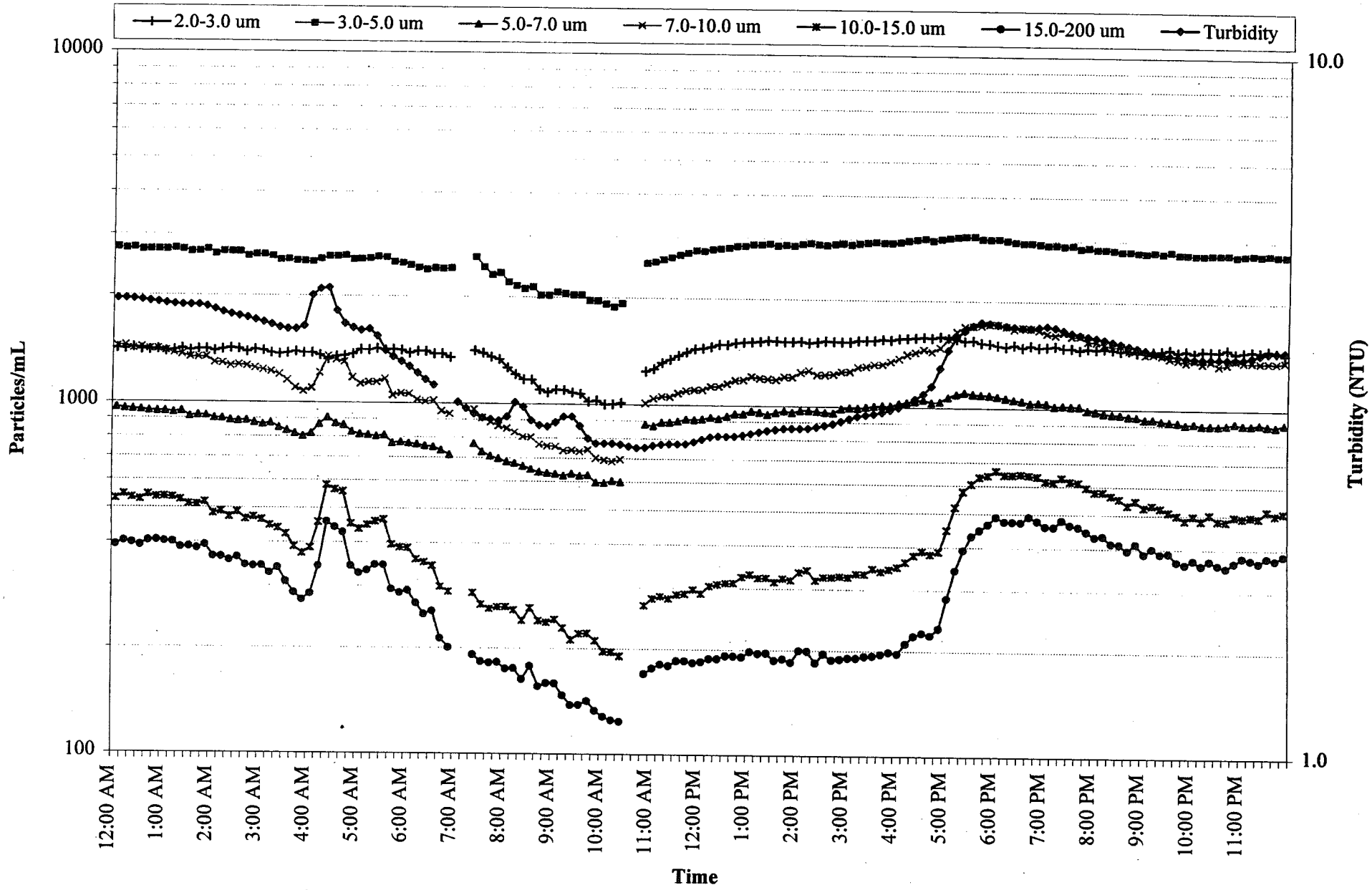

Fig. 1 (c) Scatter plot of particle counts and turbidities, 3/11/99

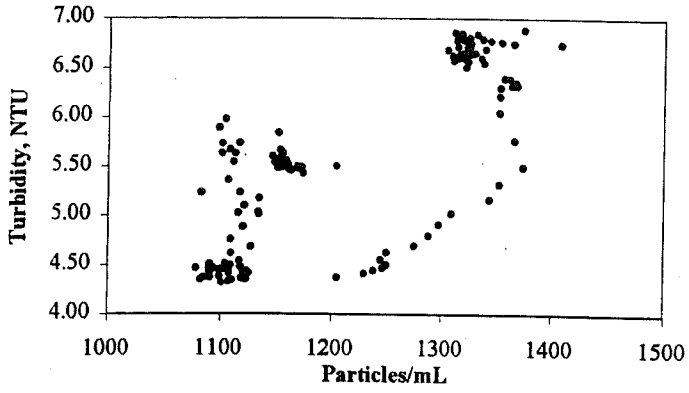

2.0-3.0 microns

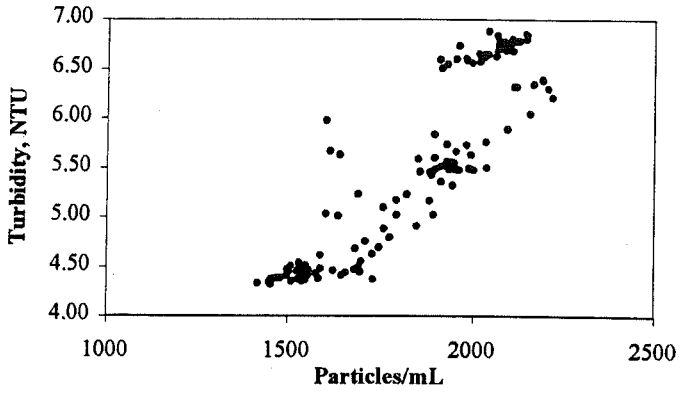

7.0-10.0 microns

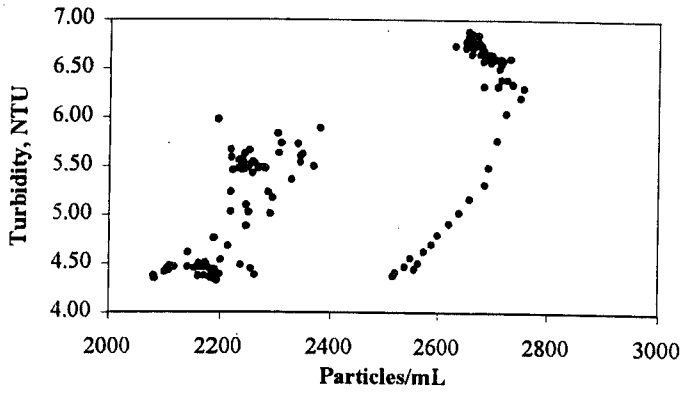

3.0-5.0 microns

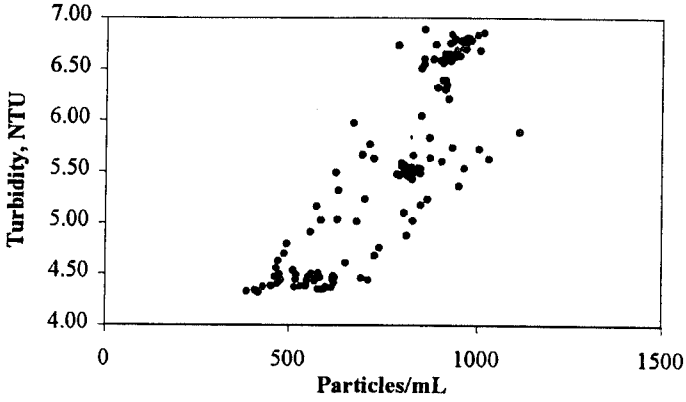

10.0-15.0 microns

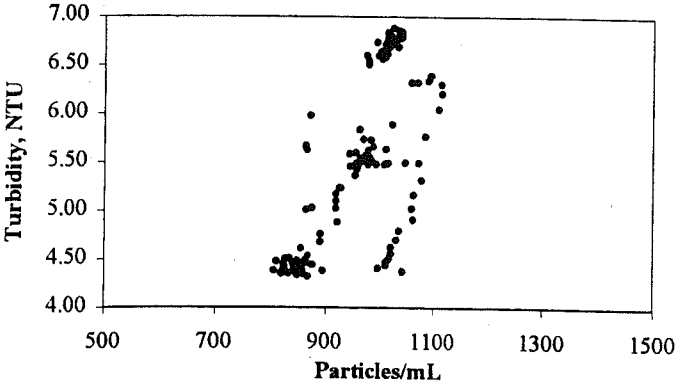

5.0-7.0 microns

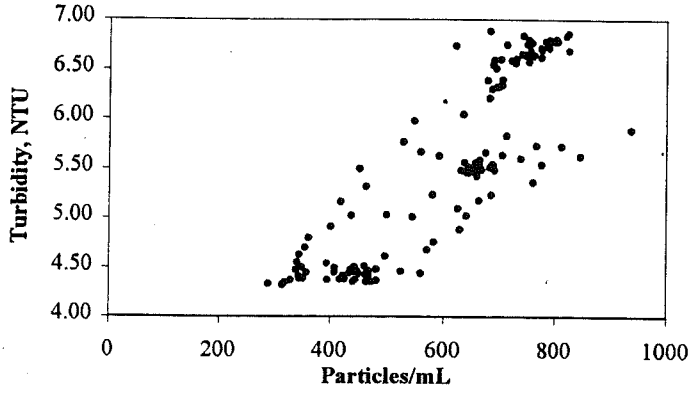

15.0-200.0 microns

Fig. 2 (c) Scatter plot of particle counts and turbidities, 3/12/99

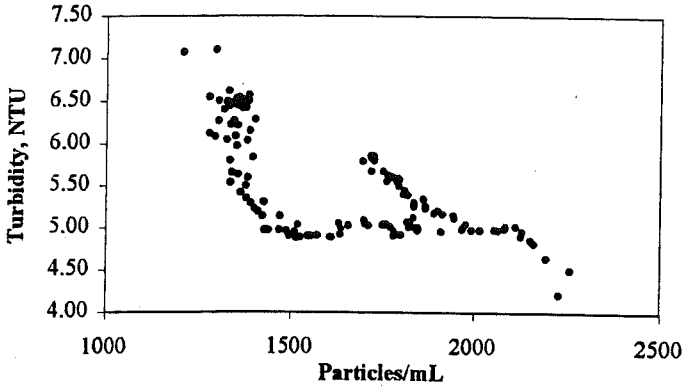

2.0-3.0 microns

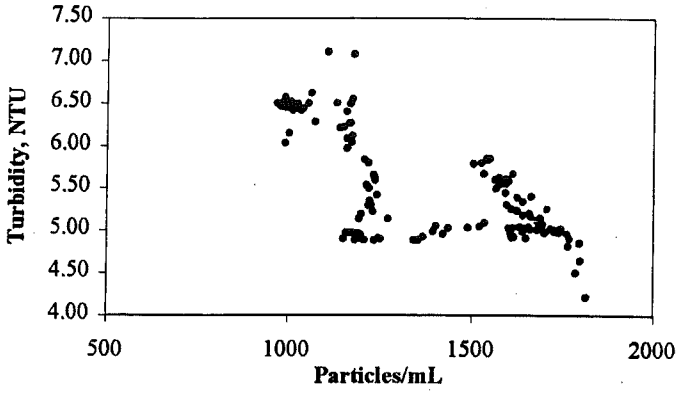

7.0-10.0 microns

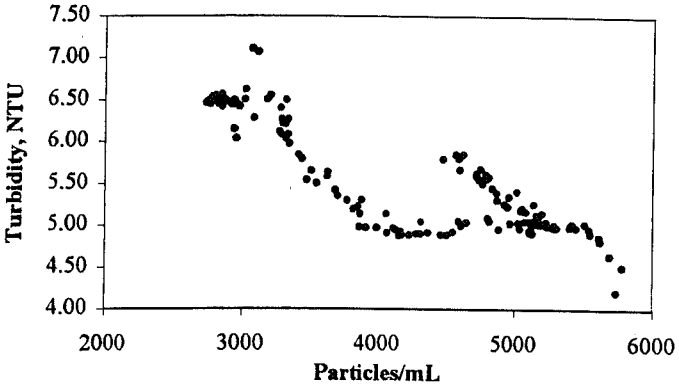

3.0-5.0 microns

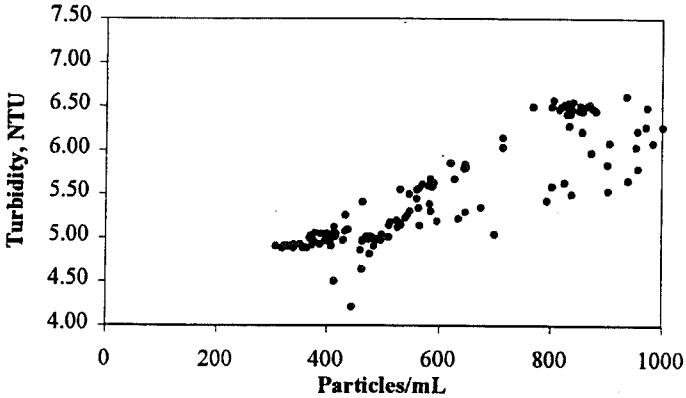

10.0-15.0 microns

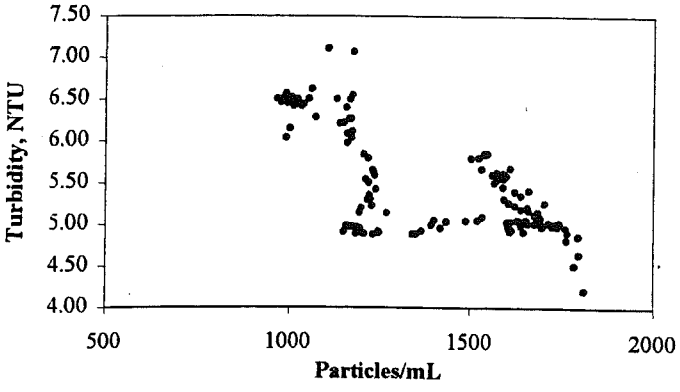

5.0-7.0 microns

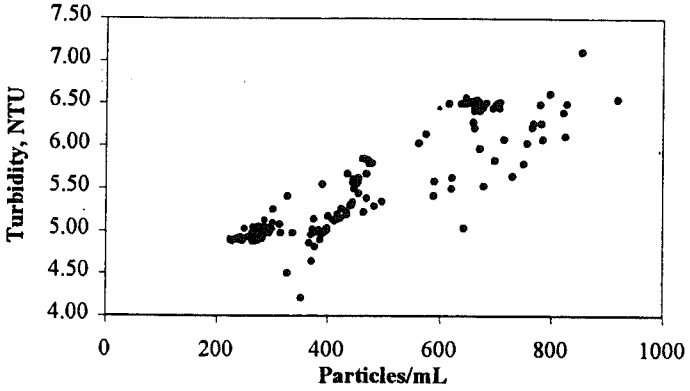

15.0-200.0 microns

Fig. 3 (c) Scatter plot of particle counts and turbidities, 3/13/99

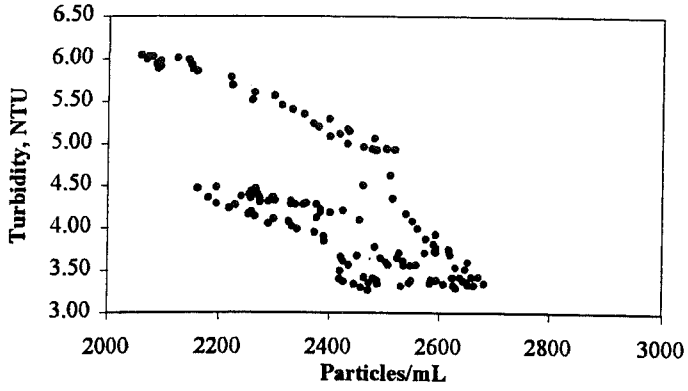

2.0-3.0 microns

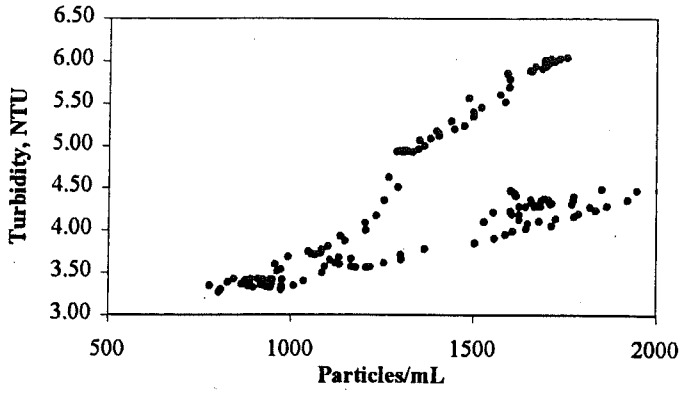

7.0-10.0 microns

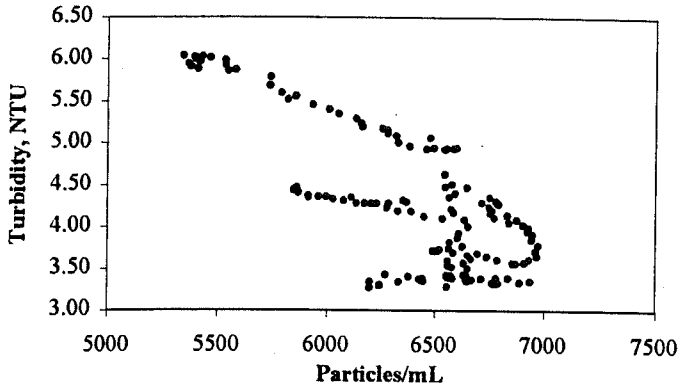

3.0-5.0 microns

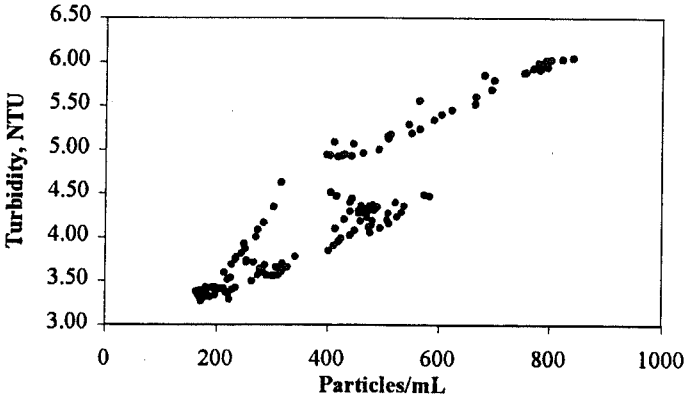

10.0-15.0 microns

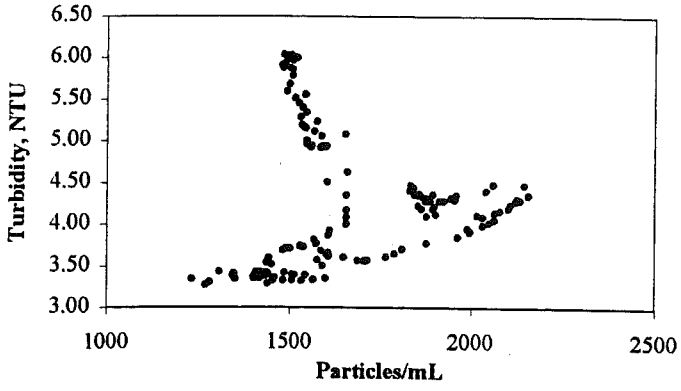

5.0-7.0 microns

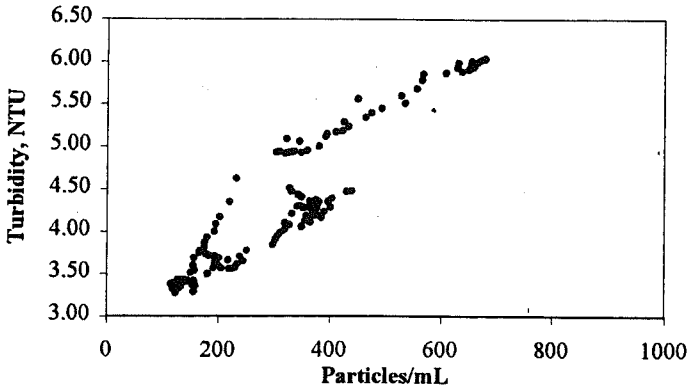

15.0-200.0 microns

Fig. 4 (c) Scatter plot of particle counts and turbidities, 3/14/99

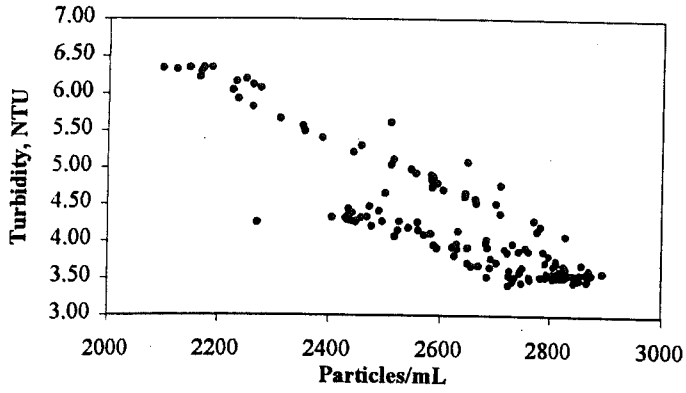

2.0-3.0 microns

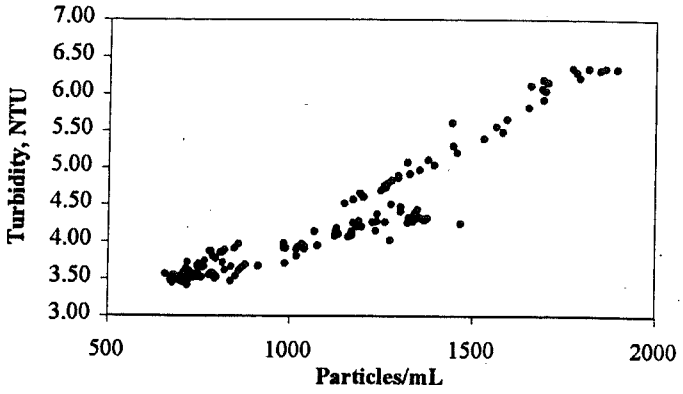

7.0-10.0 microns

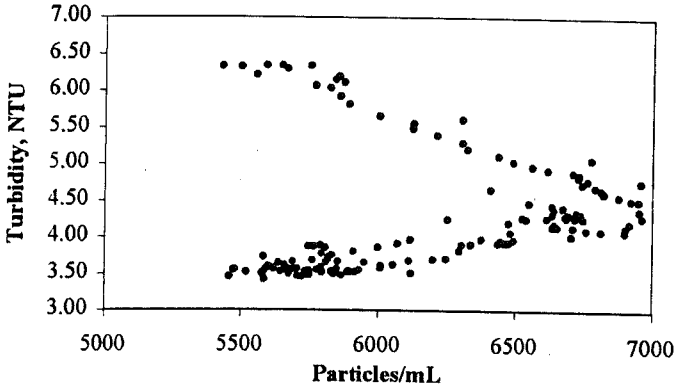

3.0-5.0 microns

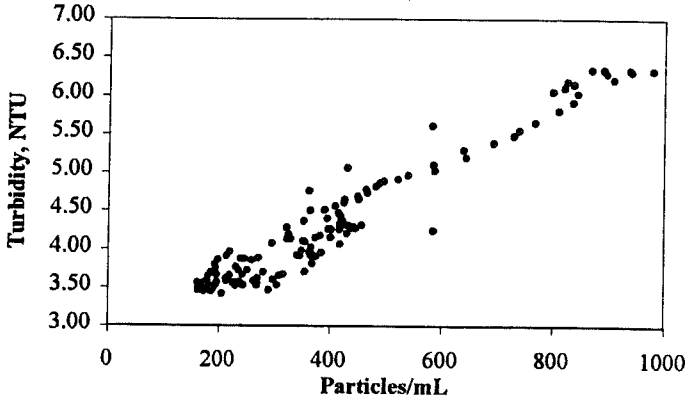

10.0-15.0 microns

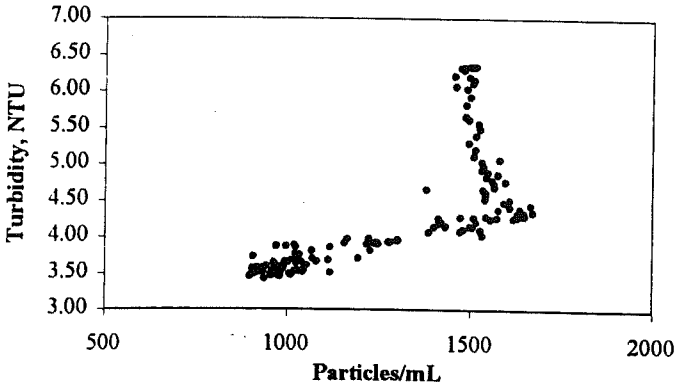

5.0-7.0 microns

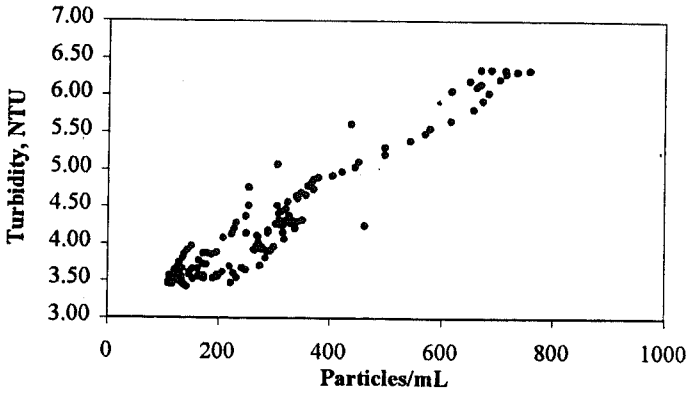

15.0-200.0 microns

Fig. 5 (c) Scatter plot of particle counts and turbidities, 3/15/99

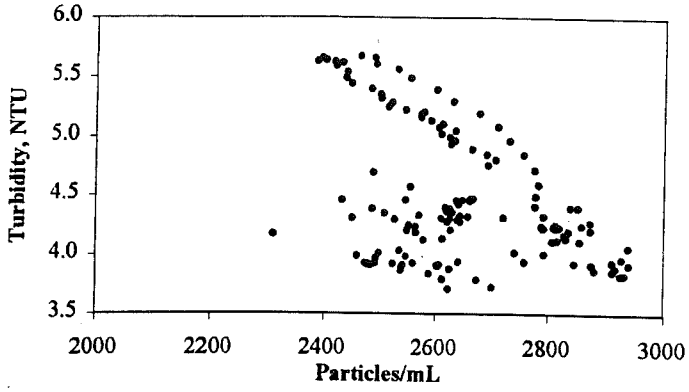

2.0-3.0 microns

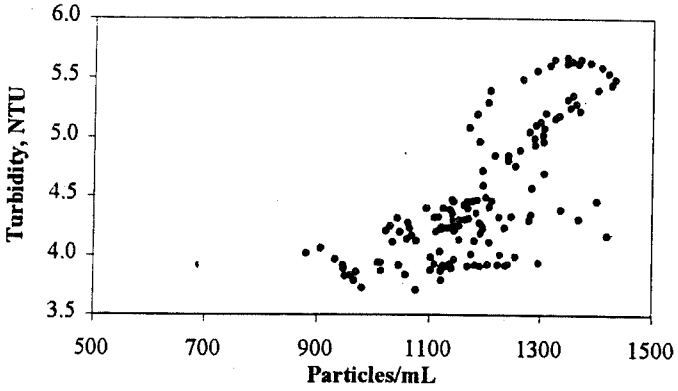

7.0-10.0 microns

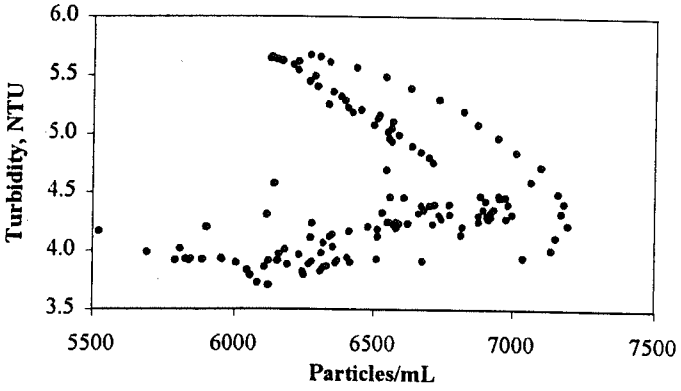

3.0-5.0 microns

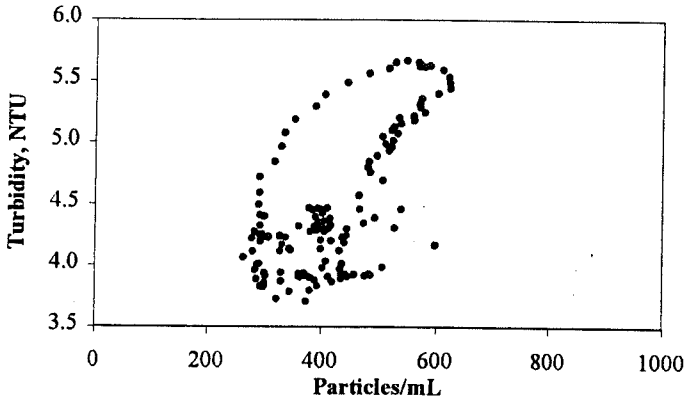

10.0-15.0 microns

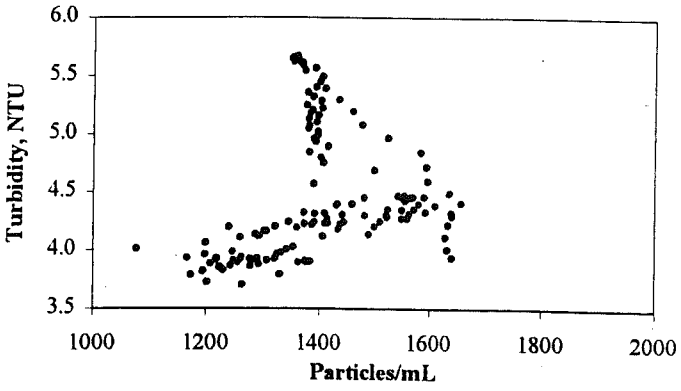

5.0-7.0 microns

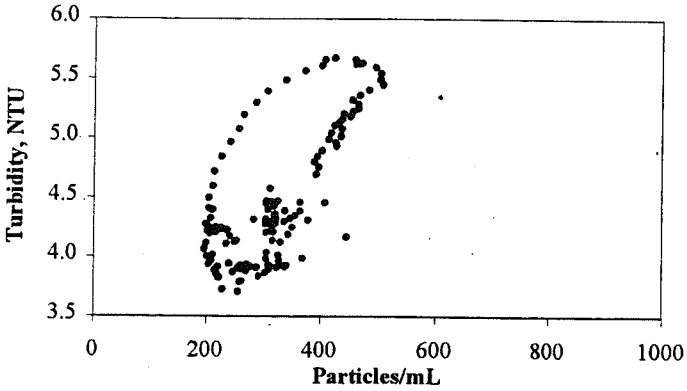

15.0-200.0 microns

Fig. 6 (c) Scatter plot of particle counts and turbidities, 3/16/99

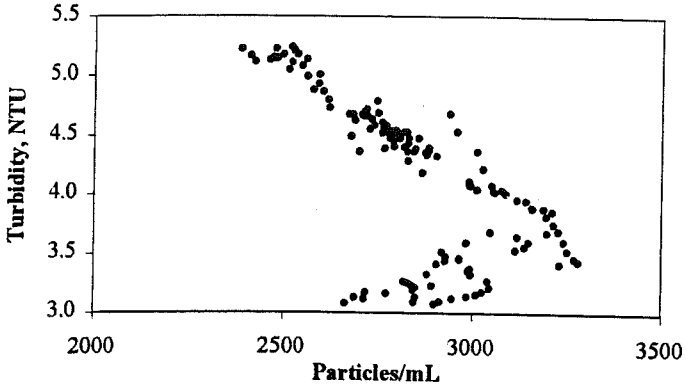

2.0-3.0 microns

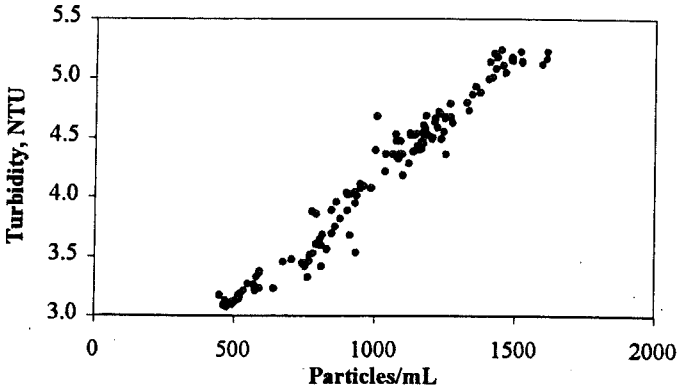

7.0-10.0 microns

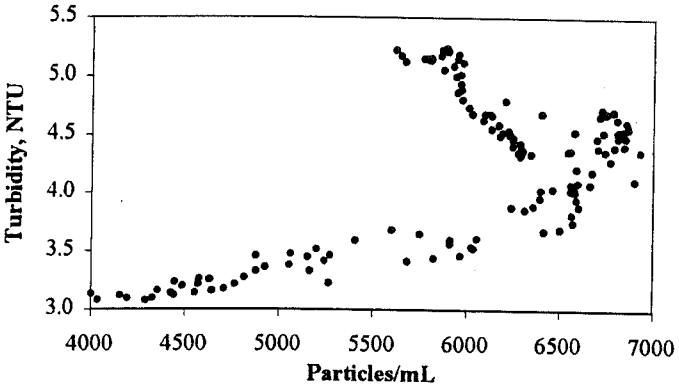

3.0-5.0 microns

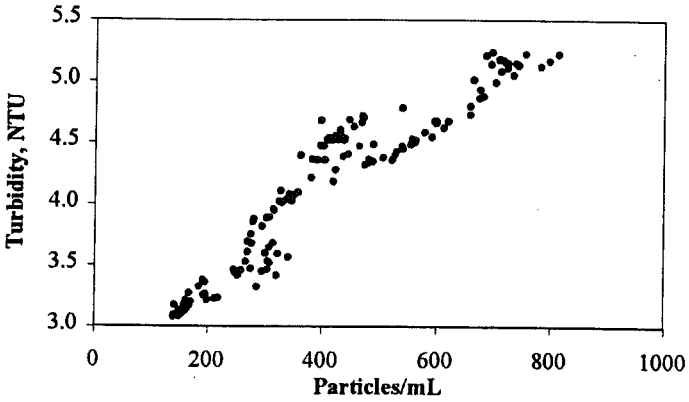

10.0-15.0 microns

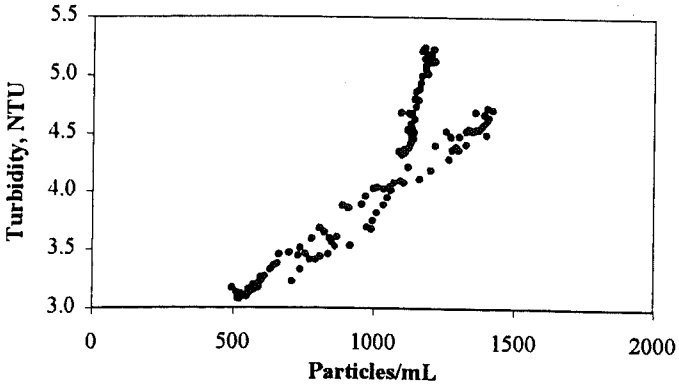

5.0-7.0 microns

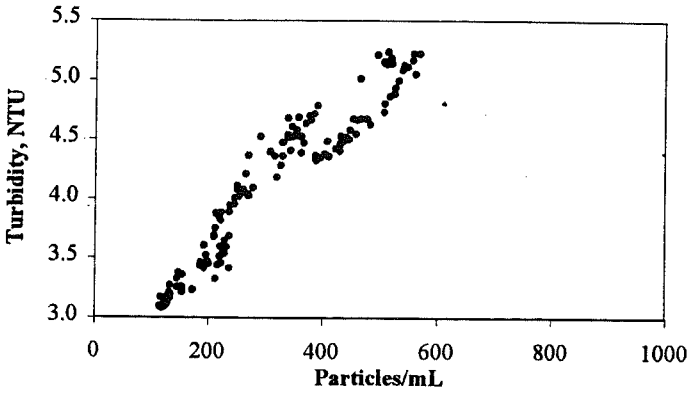

15.0-200.0 microns

Fig. 7 (c) Scatter plot of particle counts and turbidities, 3/17/99

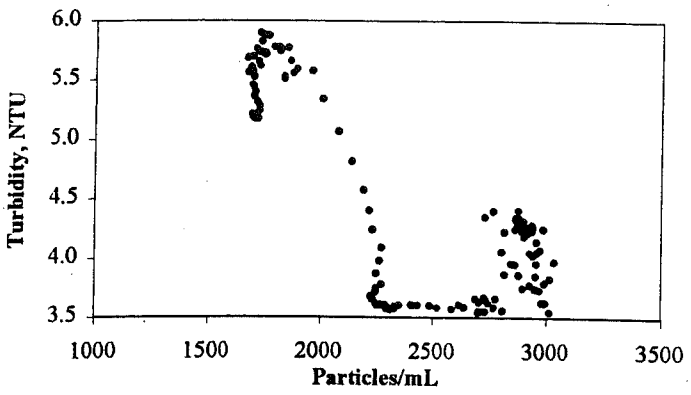

2.0-3.0 microns

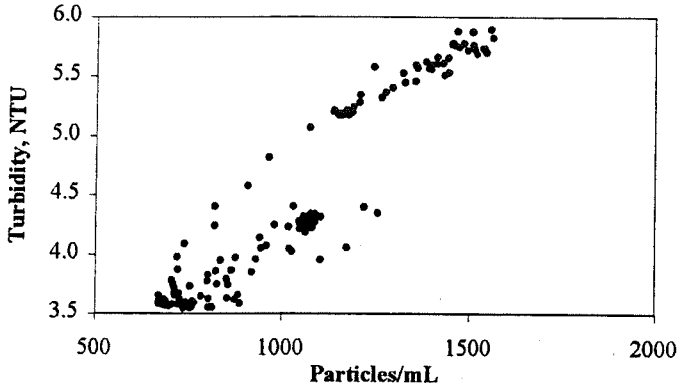

7.0-10.0 microns

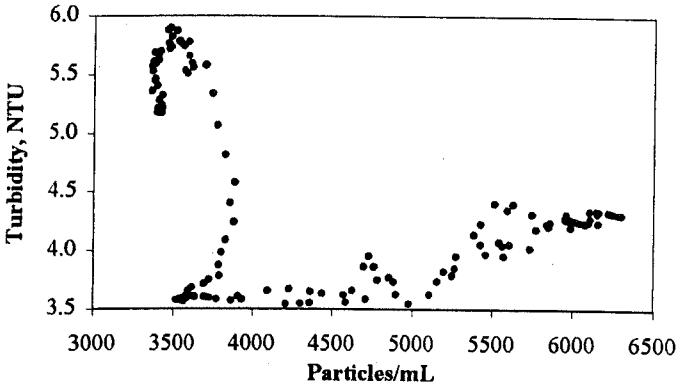

3.0-5.0 microns

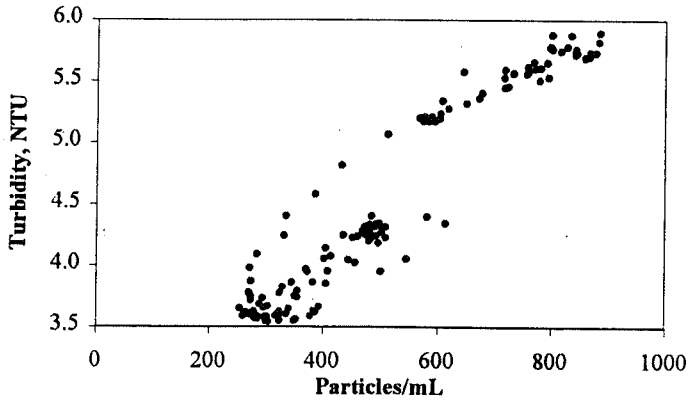

10.0-15.0 microns

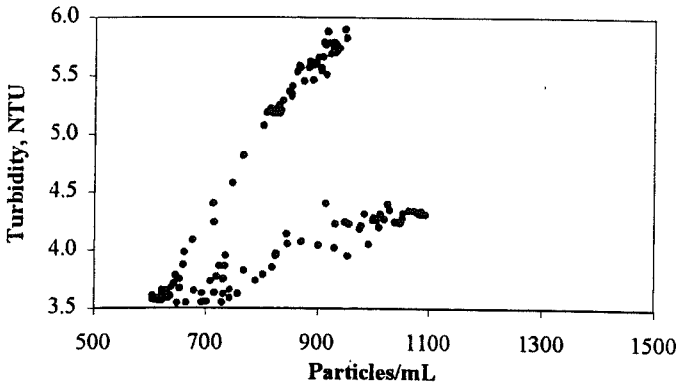

5.0-7.0 microns

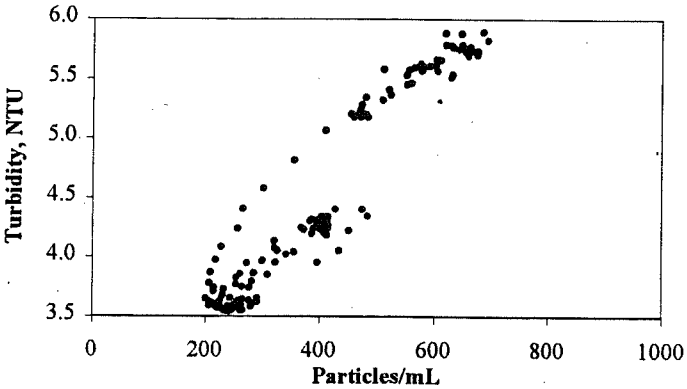

15.0-200.0 microns

Fig. 8 (c) Scatter plot of particle counts and turbidities, 3/18/99

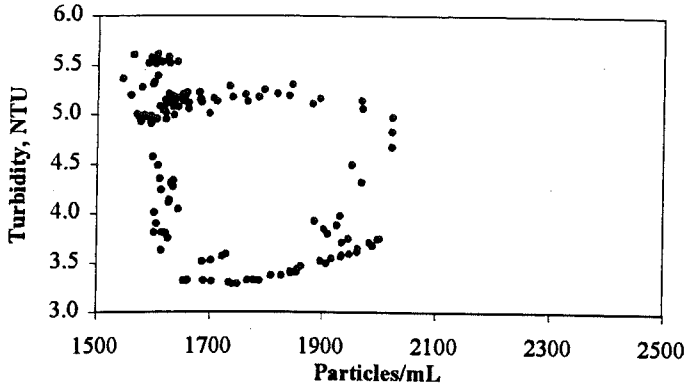

2.0-3.0 microns

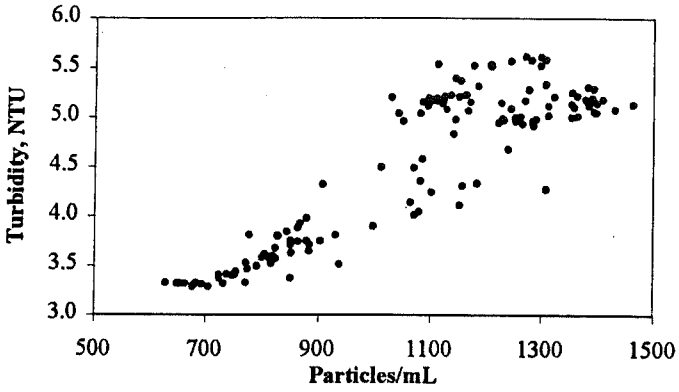

7.0-10.0 microns

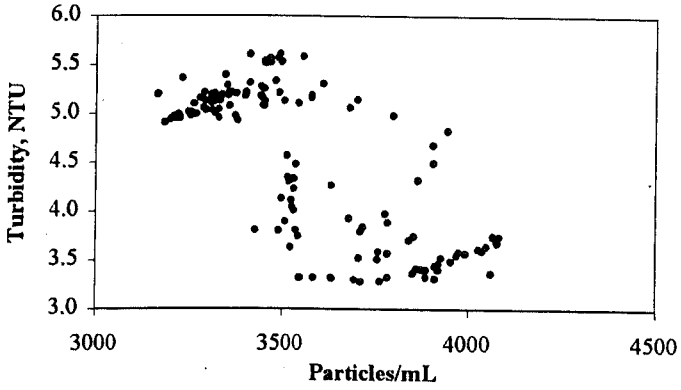

3.0-5.0 microns

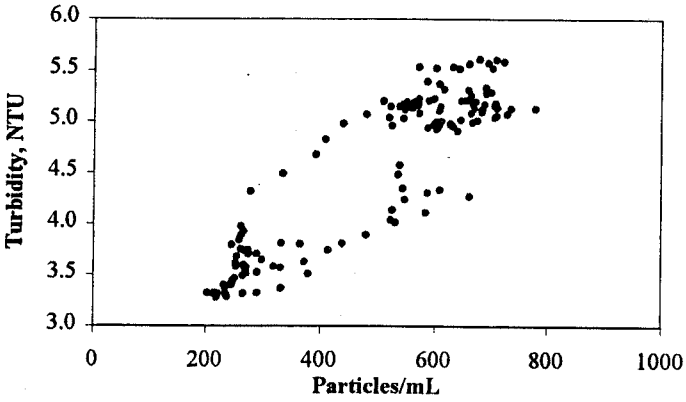

10.0-15.0 microns

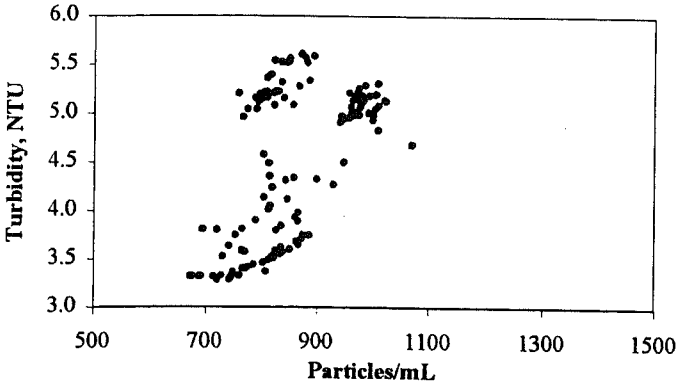

5.0-7.0 microns

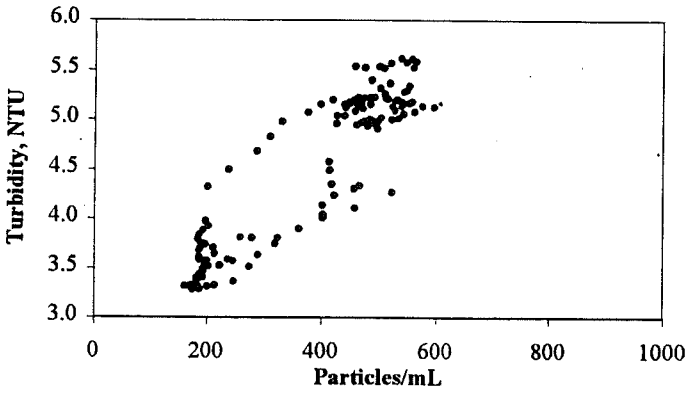

15.0-200.0 microns

Fig. 9 (c) Scatter plot of particle counts and turbidities, 3/19/99

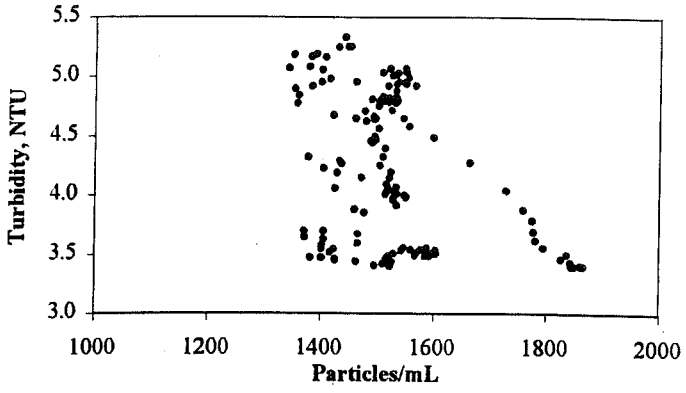

2.0-3.0 microns

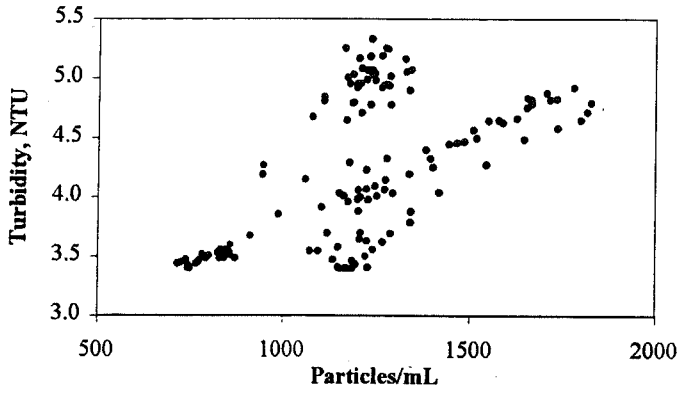

7.0-10.0 microns

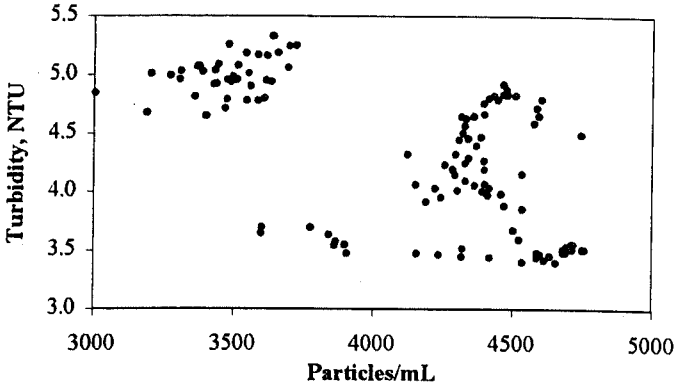

3.0-5.0 microns

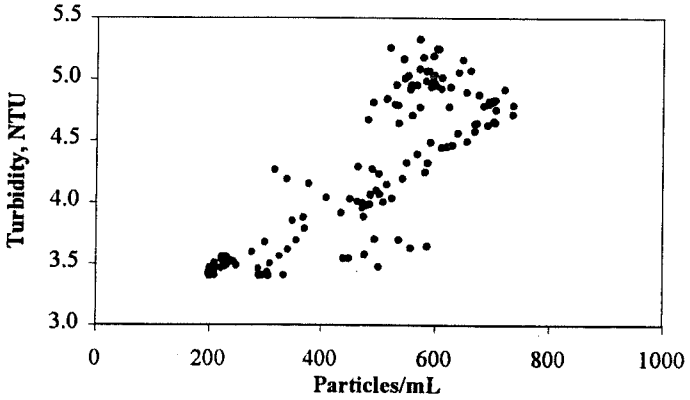

10.0-15.0 microns

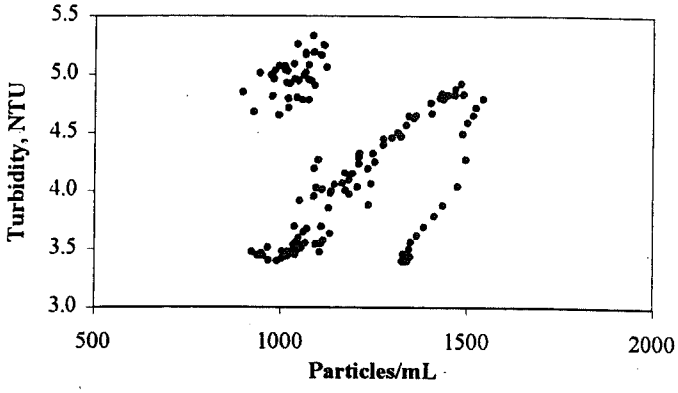

5.0-7.0 microns

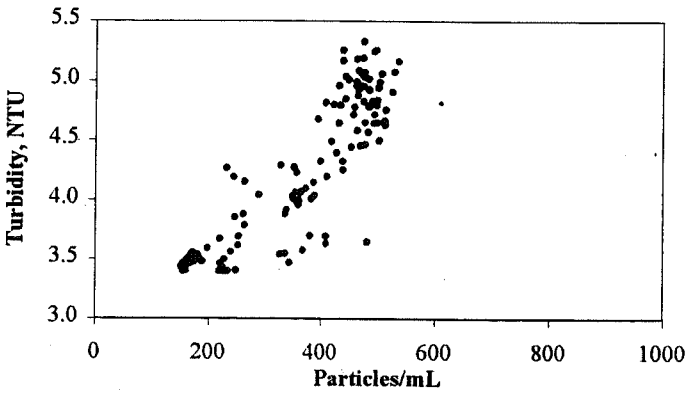

15.0-200.0 microns

Fig. 10 (c) Scatter plot of particle counts and turbidities, 3/20/99

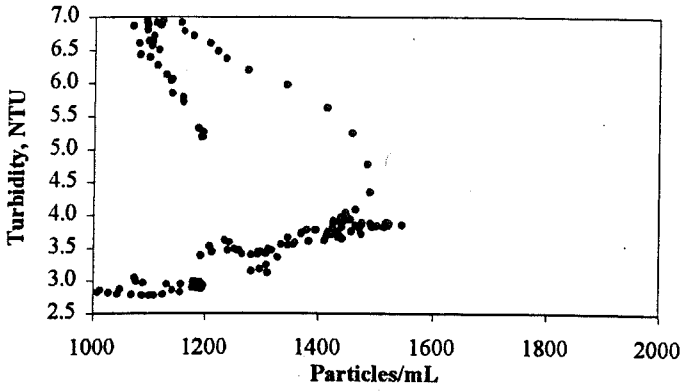

2.0-3.0 microns

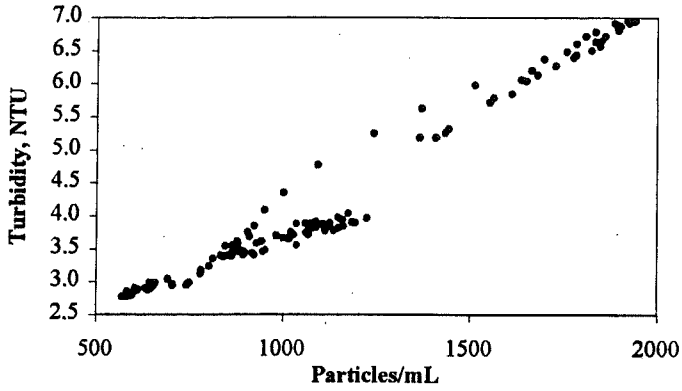

7.0-10.0 microns

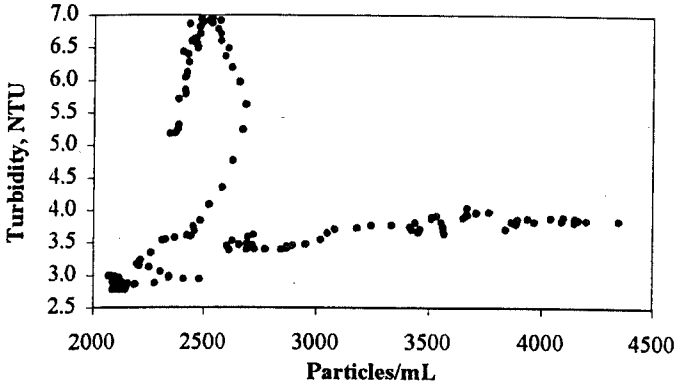

3.0-5.0 microns

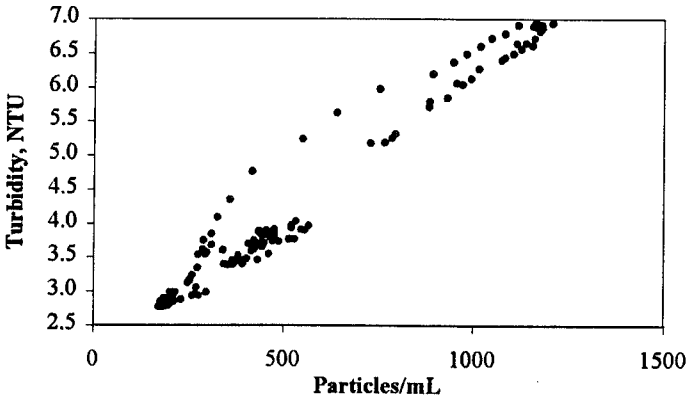

10.0-15.0 microns

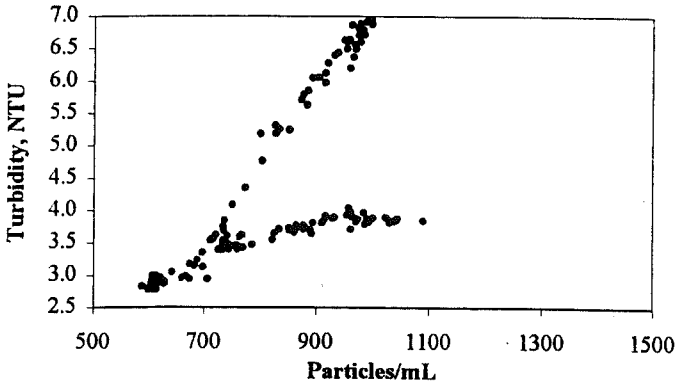

5.0-7.0 microns

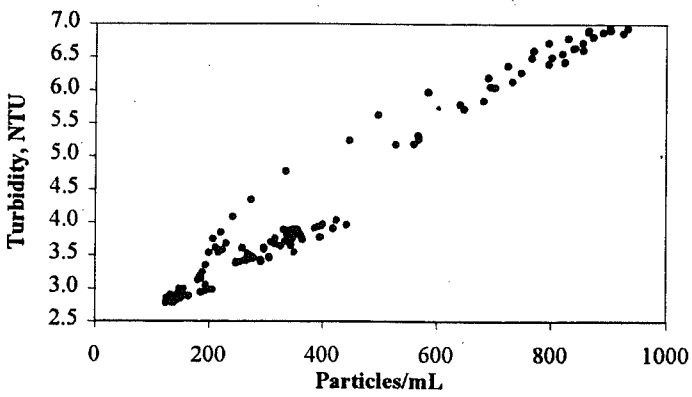

15.0-200.0 microns

Fig. 11 (c) Scatter plot of particle counts and turbidities, 3/21/99

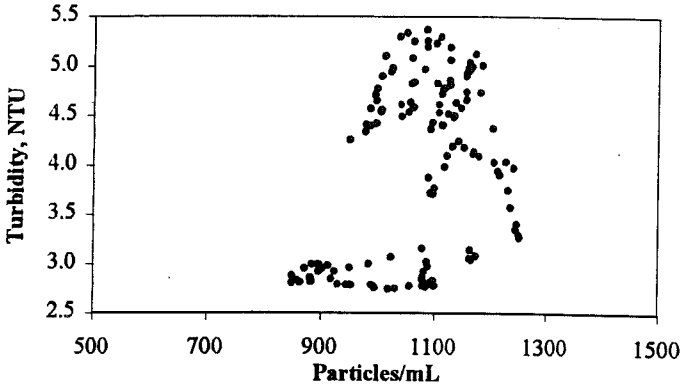

2.0-3.0 microns

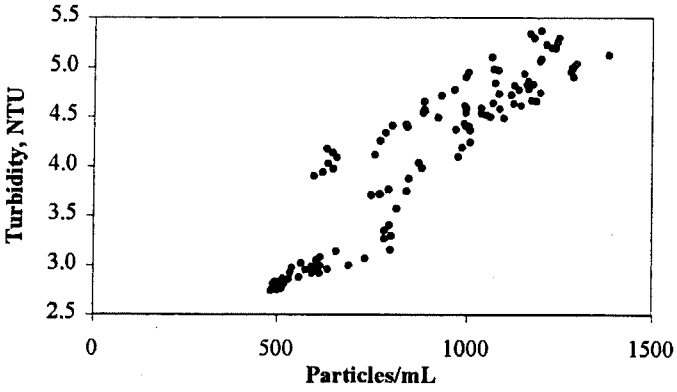

7.0-10.0 microns

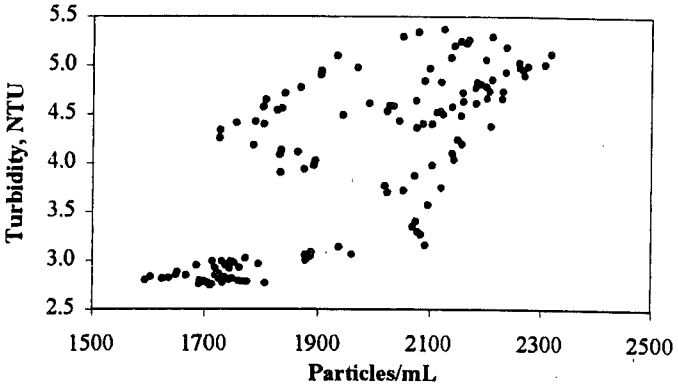

3.0-5.0 microns

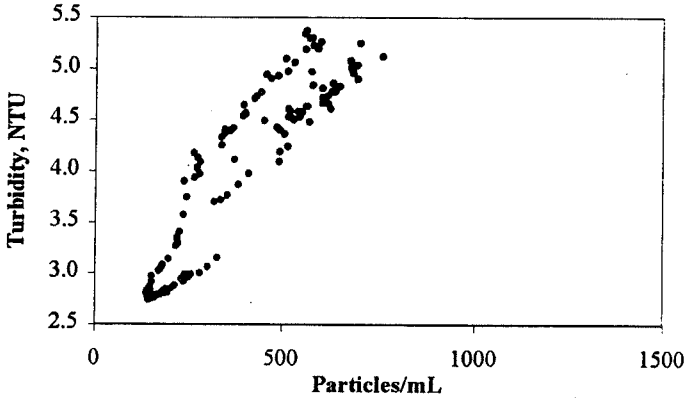

10.0-15.0 microns

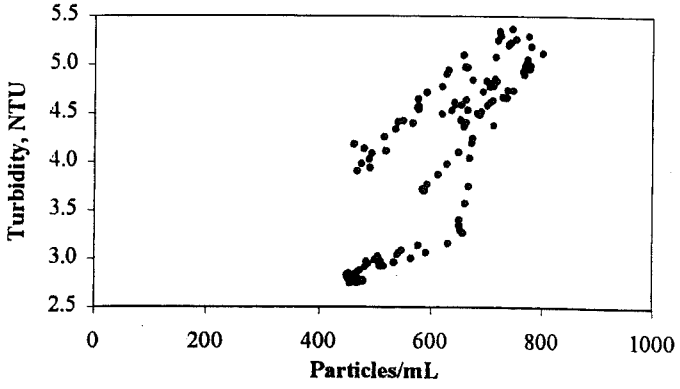

5.0-7.0 microns

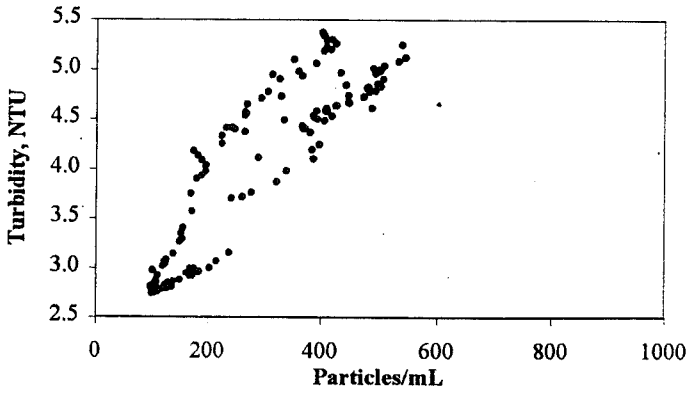

15.0-200.0 microns

Fig. 12 (c) Scatter plot of particle counts and turbidities, 3/22/99

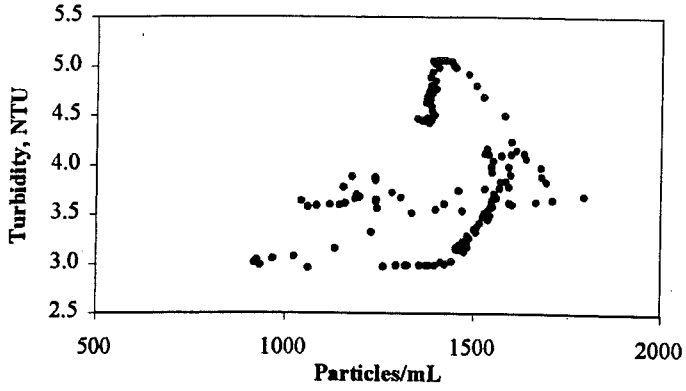

2.0-3.0 microns

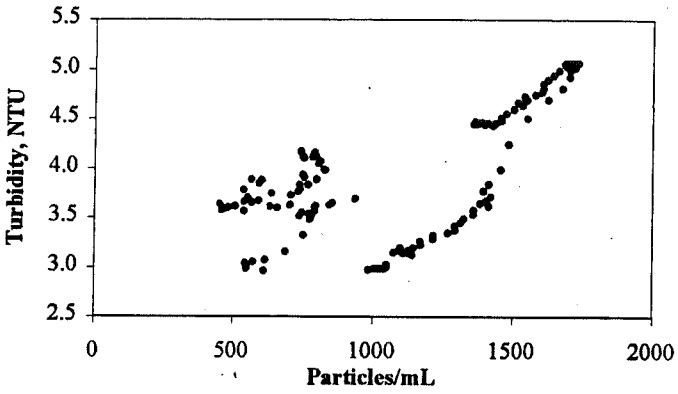

7.0-10.0 microns

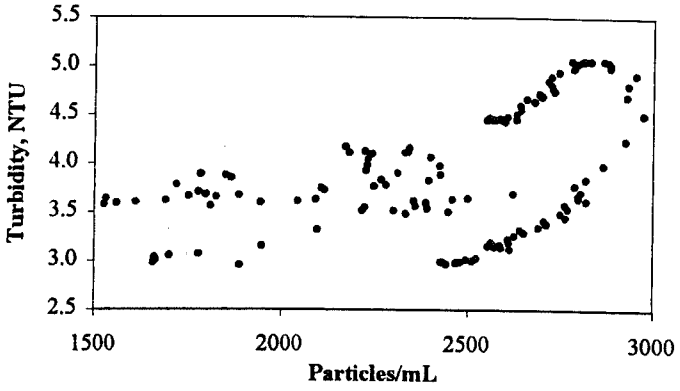

3.0-5.0 microns

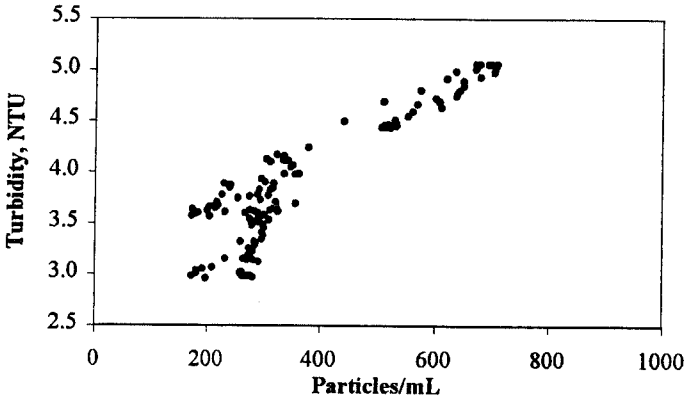

10.0-15.0 microns

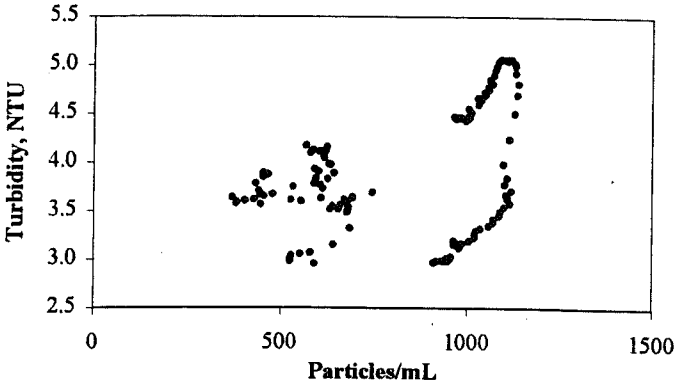

5.0-7.0 microns

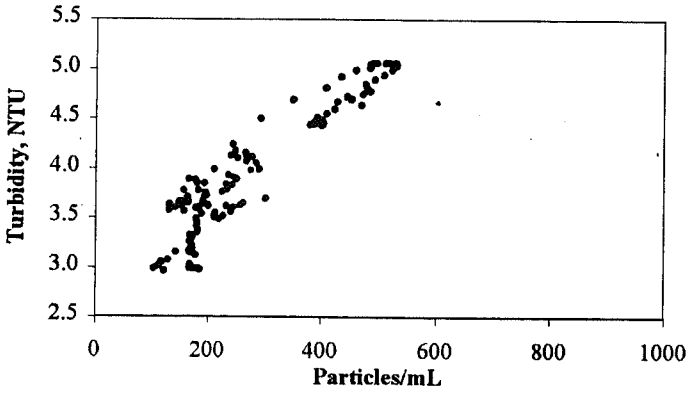

15.0-200.0 microns

Fig. 13 (c) Scatter plot of particle counts and turbidities, 3/23/99

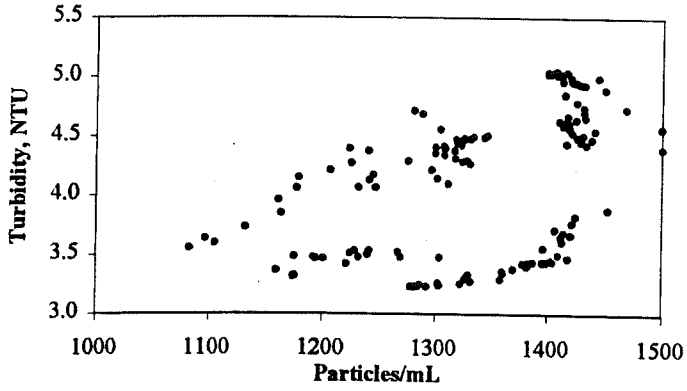

2.0-3.0 microns

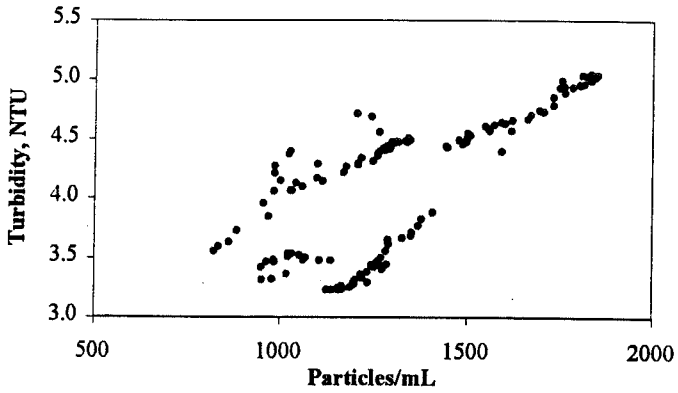

7.0-10.0 microns

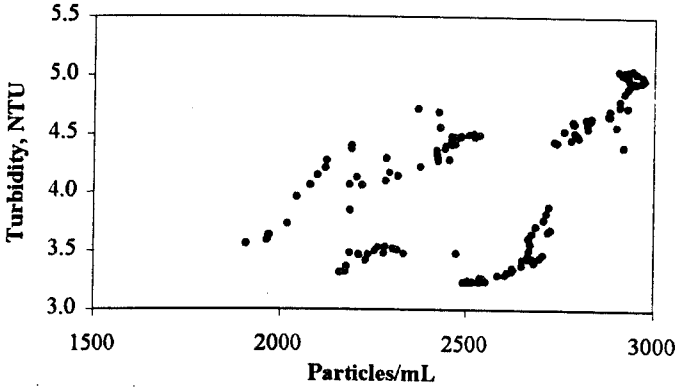

3.0-5.0 microns

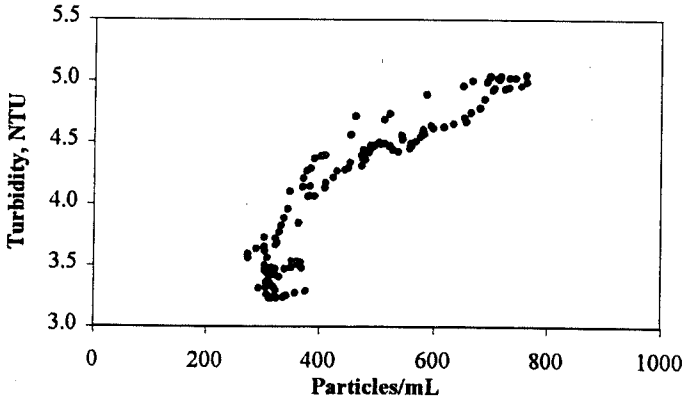

10.0-15.0 microns

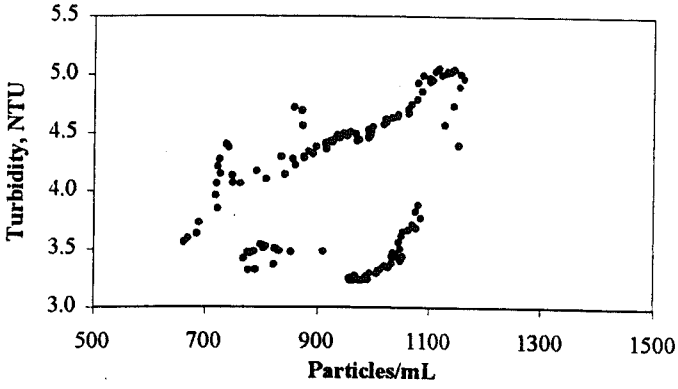

5.0-7.0 microns

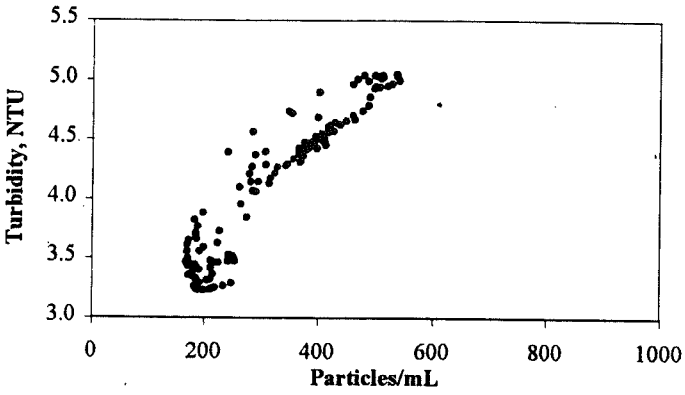

15.0-200.0 microns

Fig. 14 (c) Scatter plot of particle counts and turbidities, 3/24/99

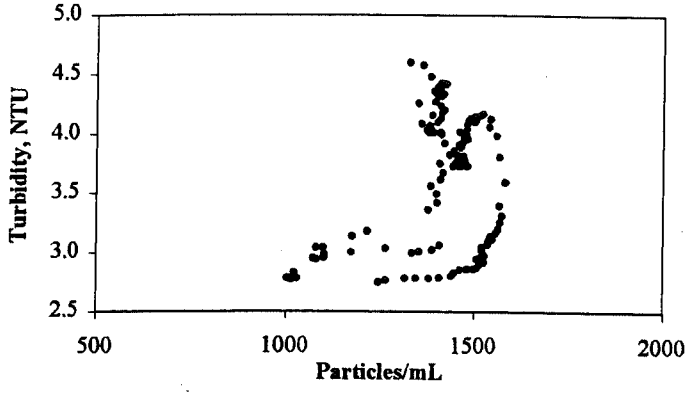

2.0-3.0 microns

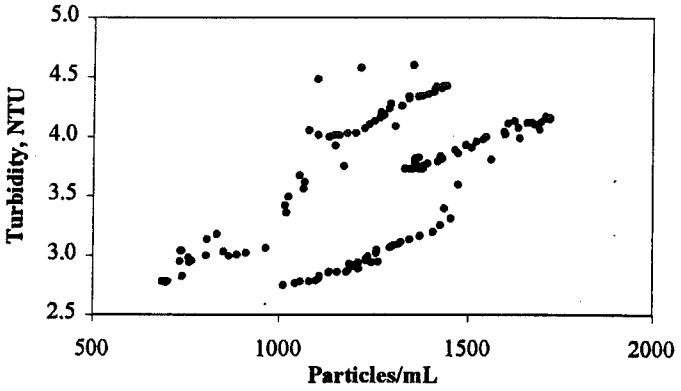

7.0-10.0 microns

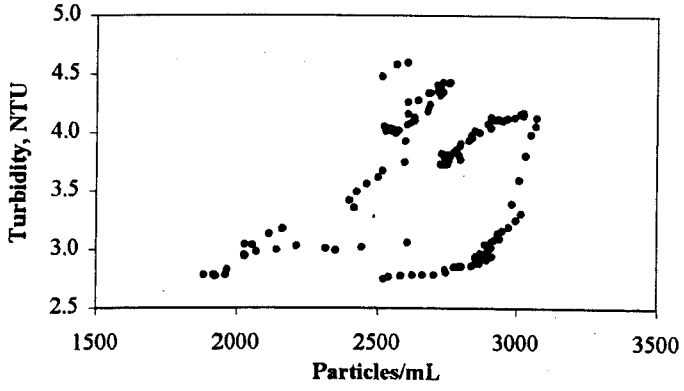

3.0-5.0 microns

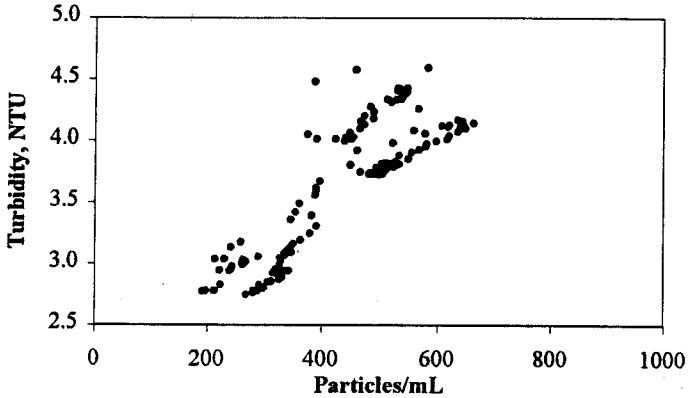

10.0-15.0 microns

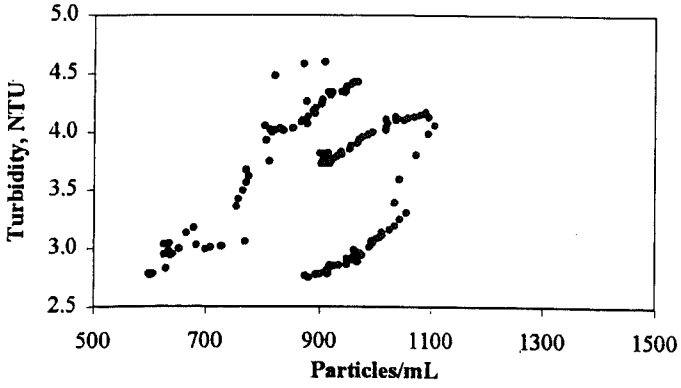

5.0-7.0 microns

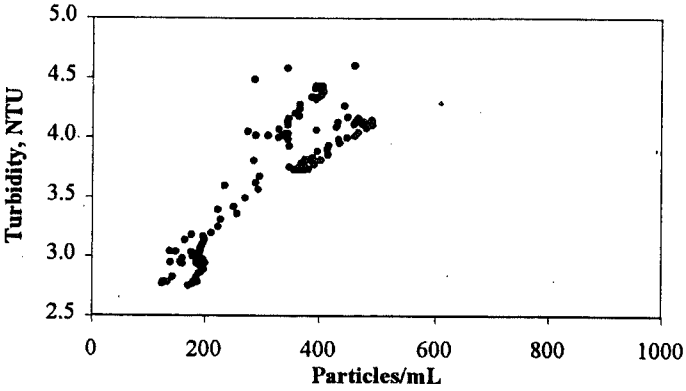

15.0-200.0 microns

Table 1. Correlation Coefficients of particle counts vs. turbidities for different particle size ranges

Size ranges	2.0-3.0	3.0-5.0	5.0-7.0	7.0-10.0	10.0-15.0	15.0-200
	Correlation coefficients					
3/11/99	0.77	0.77	0.70	0.89	0.87	0.86
3/12/99	-0.71	-0.84	-0.72	0.84	0.89	0.89
3/13/99	-0.75	-0.78	0.02	0.67	0.93	0.94
3/14/99	-0.88	0.14	0.71	0.94	0.97	0.96
3/15/99	-0.44	0.10	0.21	0.74	0.66	0.71
3/16/99	-0.68	0.63	0.88	0.98	0.94	0.96
3/17/99	-0.77	-0.40	0.54	0.94	0.96	0.95
3/18/99	-0.46	-0.74	0.55	0.88	0.90	0.91
3/19/99	-0.42	-0.69	0.06	0.61	0.84	0.89
3/20/99	-0.25	-0.06	0.68	0.98	0.98	0.98
3/21/99	0.34	0.77	0.85	0.94	0.92	0.90
3/22/99	0.19	0.45	0.37	0.65	0.90	0.93
3/23/99	0.45	0.50	0.36	0.75	0.92	0.94
3/24/99	0.26	0.30	0.36	0.63	0.87	0.90
ave ± std	-0.24±0.54	0.01±0.60	0.40±0.42	0.82±0.14	0.90±0.08	0.91±0.07